IEEE Access
Multidisciplinary | Rapid Review | Open Access Journal

Received 11 June 2022, accepted 29 July 2022, date of publication 1 August 2022, date of current version 10 August 2022.

Digital Object Identifier 10.1109/ACCESS.2022.3195892

RESEARCH ARTICLE

Robust Parameters Tuning of Different Power System Stabilizers Using a Quantum Artificial Gorilla Troops Optimizer

MAHMOUD A. EL-DABAH[1], MOHAMED H. HASSAN[2], SALAH KAMEL[2], AND HOSSAM M. ZAWBAA[3,4]

[1]Electrical Engineering Department, Faculty of Engineering, Al-Azhar University, Cairo 11651, Egypt
[2]Department of Electrical Engineering, Faculty of Engineering, Aswan University, Aswan 81542, Egypt
[3]Faculty of Computers and Artificial Intelligence, Beni-Suef University, Beni Suef 62511, Egypt
[4]CeADAR Irelands Center for Applied AI, Technological University Dublin, Dublin, D7 EWV4, Ireland

Corresponding author: Hossam M. Zawbaa (hossam.zawbaa@gmail.com)

This work was supported by the National Research and Development Agency of Chile (ANID) under Grant ANID/Fondap/15110019. The work of Hossam M. Zawbaa was supported by the European Union's Horizon 2020 Research and Enterprise Ireland under Marie Skłodowska-Curie Grant 847402.

ABSTRACT Electrical power system abnormalities may have several negative consequences on its stable operation. As a result, preserving its stability under such operational states has become an ongoing challenge for power engineers. PSSs are created as auxiliary controllers to address the instability issues produced upon disturbances. They dampen the oscillations induced by the disturbances by giving the system the necessary damping torque. This research aims at presenting a comprehensive study for the optimum tuning of power system stabilizer (PSS) of different structures. This aim is accomplished with the help of a novel modified optimization algorithm called Quantum Artificial Gorilla Troops Optimizer. The modified optimizer's validation is first investigated with the well-known benchmark optimization functions and shows superiority over Gorilla Troops Optimizer and competitive algorithms. The research is extended to the application of the optimum tuning of various PSS structures of the single machine to the infinite bus model. The proposed optimization algorithm shows fast convergence over investigated optimization algorithms. Moreover, the Tilt-integral-derivative based PSS shows better performance characteristics in terms of lower settling time and lower maximum and undershoot values over the conventional lead-lag PSS, dual input PSS, and fractional-order proportional-integral-derivative based PSS.

INDEX TERMS Power system stabilizer, tilt-integral-derivative, quantum artificial gorilla troops optimizer, dual input PSS, lead-lag PSS.

NOMENCLATURE

PSS:	Power system stabilizer.
CPSS:	Conventional lead-lag PSS.
SMIB:	Single machine to the infinite bus model.
FOPID-PSS:	Fractional-order proportional integral-derivative based PSS.
AVR:	Automatic voltage regulator.
ITAE:	Integral of time absolute error.
T_m:	Mechanical torque.
T_s:	Simulation period.
GX:	Gorilla candidate position.
DIPSS:	Dual input PSS.
TID:	Tilt-integral-derivative.
GTO:	Artificial Gorilla Troops Optimizer.
QGTO:	Quantum Artificial Gorilla Troops Optimizer.
MOS:	Maximum overshoot.
MUS:	Maximum undershoot.
STD:	Standard deviation.
$\Delta\omega$:	Rotor speed deviation.
$X()$:	Current vector of the gorilla position.

The associate editor coordinating the review of this manuscript and approving it for publication was Md. Rabiul Islam.

$X_r()$: A member of the gorillas randomly selected
$X_{silverback}$: Best solution.
it: Current iteration.
$r_{1,2,3,4}$: Random values ranging from 0 to 1.
lb & ub: Lower and upper bounds of the variables.

N: The total number of gorillas.
$Maxit$: Maximum iterations.
$Mbest$: Mean best of the population.

I. INTRODUCTION

A. BACKGROUND AND CHALLENGES

Electrical power systems are complex interconnected networks that aim to supply electric loads with the required level of quality and with minimum interruptions. Like any dynamic system, the electrical power systems are subjected to disturbances over their operations. Preserving power systems' reliability and security necessitate the need for comprehensive analysis. With the growing demand for electrical energy, the transmission lines can be heavily loaded. As a result, the power system will operate closer to the small-signal stability margins. One of the small-signal stability solicitudes is the power system oscillations that are not adequately dampened. Mechanical power variations caused by loading disturbance can cause low-frequency oscillations in local mode or interarea [1]. The automatic voltage regulator's (AVRs) primary duty is to continuously regulate the generator excitation level in response to changes in generator terminal voltage. The fast-acting AVR is salutary in enhancing the synchronizing torque component, but lamentably, the negative damping action is one of its disadvantages [2]. Resolving this conflict can be attained with the help of power system stabilizers (PSS) which enhance damping torque to damp-out low-frequency oscillations. In [3], the IEEE has standardized the PSS types model that is used in industry. Over the recent decades, numerous stabilizers and controllers have been deployed.

B. LITERATURE SURVEY

For the design of PSS, various methodologies were employed, such as self-tuning regulators, pole shifting, and pole location. Nonetheless, these methodologies encounter severe calculations that require a long time for computer processing [4]. As an alternative methodology, machine learning approaches can be utilized. Unfortunately, it requires data collection that covers a broad range of operating situations in addition to the long consumed time in system training with suitable data sets [5]. Overcoming these shortcomings as well as getting along with the merits of using the metaheuristic optimization algorithms like escaping from local optima, the PSS can be optimally tuned efficiently. Recently, a significant number of such algorithms have been published like, Chaotic Particle Swarm Optimization [6], whale optimization algorithm [7], enhanced whale optimization algorithm [8], improved Moth flame optimization [9], An antlion optimization [10], Slime Mould Algorithm [11], Coyote Optimization Algorithm [12], Henry Gas Solubility Algorithm [13], collective decision algorithm [14], Particle Swarm Optimization [15], Cuckoo Search Algorithm [16], Salp Swarm Algorithm [17], hybrid dynamic GA-PSO algorithm [18], atom search algorithm [19], Runge Kutta optimizer [20], Genetic Algorithms [21], kidney-inspired algorithm [22], modified harmonic search algorithm [23], sine cosine algorithm [24], Harmony Search [25], farmland fertility algorithm [26]-[29], Bat Algorithm [30], Honey Bee Mating Optimization [31], Jaya Algorithm [32], [33], Grey Wolf Optimizer [34], Backtracking Search Algorithm [35], Grasshopper Optimization Approach [36], Rat Swarm Optimization[37]. Harris Hawk Optimizer[38].

The recognized fractional-order calculus-based controllers like FOPID and TID are invited for various power system applications like load frequency control[39]-[41], hybrid power system control[42],[43] microgrids frequency stability [44],[45]…etc. This is due to its remarkable potential for disturbance rejection and increased sensitivity to model parameter changes. The TID-PSS will be employed in this research. Also, its performance will be compared with the FOPID-PSS and the dual input PSS (DIPSS).

C. MOTIVATION

As per the 'No free lunch theorems for optimization', it is impractical to say which optimization technique will achieve the global optimum for all optimization problems[46]. The Artificial Gorilla Troops Optimizer (GTO) [47] is one of the recently introduced optimization algorithms. This algorithm inherits its idea from the natural social intelligence of Gorilla Troops. Owing to GTO's advantages of easy-to-implement and strong adaptability, the original GTO algorithm converges fast. However, once it gets stuck into the local optima, it will be very hard to get out from the local minima. To overcome this issue, quantum mechanics are introduced into the GTO algorithm. These suggested changes also enhance the ability of the GTO to balance exploitation and exploration for a better investigation of the solution. The proposed Quantum Artificial Gorilla Troops Optimizer (QGTO) technique depends on adopting a quantum model of the search space and operators in the GTO algorithm to achieve the best solution for the objective function. In this paper, the application of the QGTO to optimally tune various structures of PSSs is employed to prove its capability to solve such non-linear optimization problems.

D. CONTRIBUTION

The main contribution of this research can be summarized in the following points:

a) Introducing a novel optimization algorithm called QGTO.
b) Validation of the proposed optimizer through the application of the well-known benchmark functions.
c) Studying the response of CPSS, dual input, and TID-PSS to disturbances in the SMIB model.

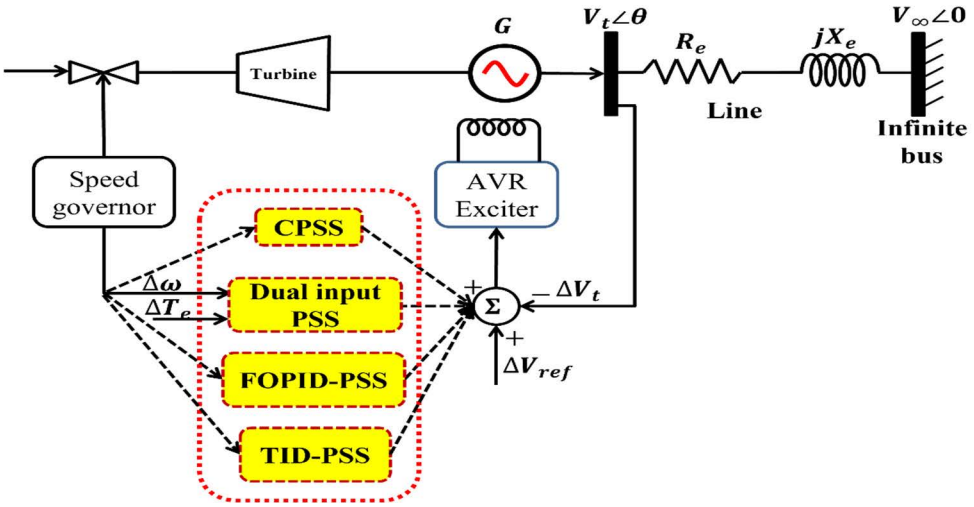

FIGURE 1. SMIB accompanied by PSS.

d) Investigating performance of the QGTO, GTO, and other optimization algorithms for the capability of optimum tuning of various structures of PSSs.

E. PAPER ORGANIZATION

The rest sections of this manuscript are shortly presented as follows. In section II, the mathematical modeling and formulation will be presented. Also, section III gives an overview of the QGTO, while sections IV and V illustrate the application of QGTO to the optimal tuning of investigated PSS structures and discuss the obtained results. Finally, section VI spots light on the main findings of this research.

II. PROBLEM MATHEMATICAL FORMULATION

This section aims at presenting the mathematical model of the single machine to the infinite bus along with the modeling of various PSSs structures. The SMIB model consists of a synchronous machine that is connected to an infinite bus through a transmission line. The synchronous machine is accompanied by the automatic voltage regulator (AVR), the exciter, and the PSS, as shown in Figure 1. In this research, the 4th order model of a synchronous machine will be employed to analyze local mode oscillations. The following set of equations can be used to mathematically model the SMIB [44]:

$$\dot{\delta} = \omega_b(\omega - 1) \tag{1}$$

$$\dot{\omega} = \frac{1}{M}(P_M - P_E - P_D) \tag{2}$$

$$\dot{E}'_q = \frac{1}{T'_{do}}\left[E_{fd} - E'_q - (x_d - x'_d)\, i_d\right] \tag{3}$$

$$\dot{E}_{fd} = \frac{1}{T_E}\left[K_A(v_{tr} - v_t + u_{PSS}) - E_{fd}\right] \tag{4}$$

$$P_E = E'_q i_q + (x_q - x'_d)\, i_d i_q \tag{5}$$

The linearized incremental models around a steady-state point are commonly used in the design of PSSs. Hence, the previous equations can be linearized as follows to constitute the well-known Heffron-Philips model with constants (K1–K6):

$$\Delta\dot{\delta} = \omega_b \Delta\omega \tag{6}$$

$$\Delta\dot{\omega} = -\frac{K1}{2H}\Delta\delta - \frac{D}{2H}\Delta\omega - \frac{K2}{2H}\Delta E'_q \tag{7}$$

$$\Delta\dot{E}'_q = \frac{K4}{T'_{do}}\Delta\delta - \frac{1}{T'_{do}K3}\Delta E'_q + \frac{1}{T'_{do}}\Delta E_{fd} \tag{8}$$

$$\Delta\dot{E}_{fd} = -\frac{k_A K5}{T_A}\Delta\delta - \frac{k_A K6}{T_A}\Delta E'_q - \frac{1}{T_A}\Delta E_{fd} + \frac{k_A}{T_A}\Delta u_{PSS} \tag{9}$$

All these equations can be arranged in a matrix form to present the state-space model as given in Eqs. (10, 11).

$$\begin{bmatrix} \Delta\dot{\delta} \\ \Delta\dot{\omega} \\ \Delta\dot{E}'_q \\ \Delta\dot{E}_{fd} \\ \Delta\dot{v}_\omega \\ \Delta\dot{u}_{PSS} \end{bmatrix} = \begin{bmatrix} 0 & \omega_b & 0 & 0 & 0 & 0 \\ -\frac{K1}{2H} & -\frac{D}{2H} & -\frac{K2}{2H} & 0 & 0 & 0 \\ \frac{K4}{T'_{do}} & 0 & -\frac{1}{T'_{do}K3} & \frac{1}{T'_{do}} & 0 & 0 \\ -\frac{k_A K5}{T_A} & 0 & -\frac{k_A K6}{T_A} & -\frac{1}{T_A} & 0 & \frac{k_A}{T_A} \\ -\frac{K_1 K_{PSS}}{2H} & 0 & -\frac{K_2 K_{PSS}}{2H} & 0 & -\frac{1}{T_W} & 0 \\ -\frac{T_1 K_1 K_{PSS}}{2HT_2} & 0 & -\frac{T_1 K_2 K_{PSS}}{2HT_2} & 0 & \frac{1}{T_2}(1 - \frac{T_1}{T_W}) & -\frac{1}{T_2} \end{bmatrix} \times \begin{bmatrix} \Delta\delta \\ \Delta\omega \\ \Delta E'_q \\ \Delta E_{fd} \\ \Delta v_\omega \\ \Delta u_{PSS} \end{bmatrix} + \begin{bmatrix} 0 & 0 \\ \frac{1}{2H} & 0 \\ 0 & 0 \\ 0 & \frac{k_A}{T_A} \\ \frac{K_{PSS}}{2H} & 0 \\ \frac{T_1 K_1 K_{PSS}}{2HT_2} & 0 \end{bmatrix} \tag{10}$$

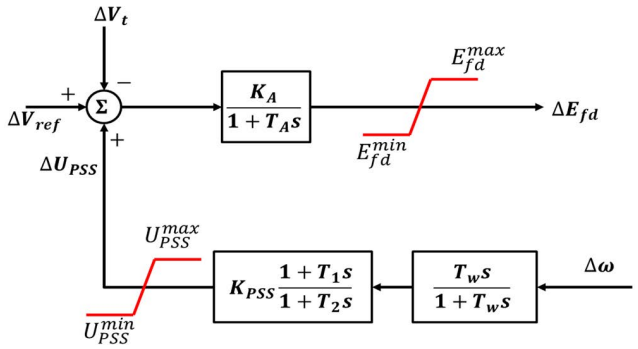

FIGURE 2. Conventional lead-lag PSS.

$$\begin{bmatrix} \Delta\omega \\ \Delta E_{fd} \\ \Delta V_t \\ \Delta T_e \end{bmatrix} = \begin{bmatrix} 0 & 1 & 0 & 0 & 0 & 0 \\ 0 & 0 & 0 & 1 & 0 & 0 \\ K3 & 0 & K6 & 0 & 0 & 0 \\ K1 & 0 & K2 & 0 & 0 & 0 \end{bmatrix} \begin{bmatrix} \Delta\delta \\ \Delta\omega \\ \Delta E'_q \\ \Delta E_{fd} \\ \Delta v_\omega \\ \Delta v_s \end{bmatrix} + \begin{bmatrix} 0 & 0 \\ 0 & 0 \\ 0 & 0 \\ 0 & 0 \end{bmatrix} \begin{bmatrix} \Delta T_m \\ \Delta E_{fd} \end{bmatrix} \tag{11}$$

As per the essential role of PSS to provide compensation for the negative damping torque component produced by the AVR, various PSSs structures will be investigated in this research.

The conventional lead-lag PSS (CPSS) is depicted in Figure 2, which is mathematically defined by:

$$\frac{\nabla u_{PSS}}{\Delta\omega} = K_{PSS} \cdot \frac{sT_w}{1 + sT_w} \cdot \frac{(1 + sT_1)}{(1 + sT_2)} \tag{12}$$

where, T_w denotes the wash-out filter time constant (10s in this research). T_1 and T_2 are phase-lead and phase lag time constants respectively.

Moreover, the FOPID and TID-based PSS will be employed for evaluation as per improved disturbance rejection capabilities and superior sensitivity to model parameter variations. The stabilization signal of both FOPID and TID-based PSSs is given in Eqs. (13) and (14). Figure 3 shows a schematic representation of the TID controller, while Figure 4 shows the block diagram of the DIPSS (i.e., the PSS3B model).

$$\nabla u_{PSS} = \left(K_P + \frac{K_I}{s^\lambda} + K_D s^\mu \right) \Delta\omega \tag{13}$$

$$\nabla u_{PSS} = \left(\frac{K_t}{s^{(\frac{1}{n})}} + \frac{K_I}{s} + K_D s \right) \Delta\omega \tag{14}$$

The rotor speed deviation ($\Delta\omega$) is employed in the fitness function to reach the optimal parameter values of investigated PSSs. As a result, the integral of time absolute error (ITAE) is used as a performance index which is given by Eq.(12) with

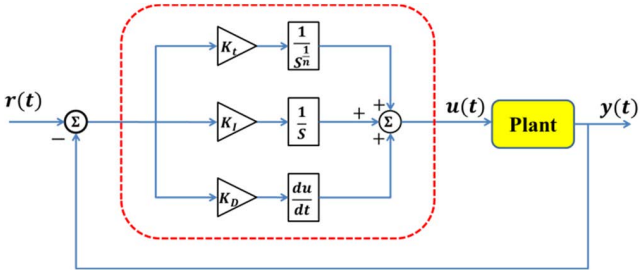

FIGURE 3. TID controller schematic diagram.

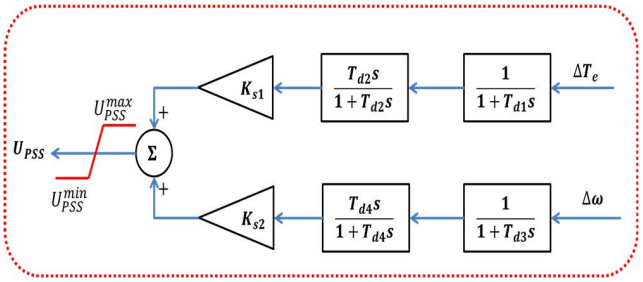

FIGURE 4. PSS3B block diagram.

T_s is the simulation period:

$$f = \int_0^{T_s} t \times |\Delta\omega| dt \tag{15}$$

To provide the appropriate stabilization signal from the PSS, it is required to tune its parameters. The QGTO will be employed for the optimum tuning of investigated PSS structures with the aid of ITSE as a fitness function. Figure 5 illustrates this process in the case of utilizing TID-based PSS.

III. THE PROPOSED APPROACH OF OPTIMIZATION

The Artificial Gorilla Troops Optimizer (GTO) algorithm is briefly presented in this section then the process of the quantum GTO (QGTO) technique is described.

A. ARTIFICIAL GORILLA TROOPS OPTIMIZER (GTO)

1) EXPLORATION PHASE

Three different operators were used in the exploration phase: Move to an unknown location to further explore the GTO algorithm. The second factor, the transition to other gorillas, increases the balance between exploration and exploitation [47]. The third factor is in the exploration phase; that is, migrating to a known location greatly increases the ability of the GTO algorithm to search for different improvement spaces. These different operators can be represented using the following equation:

$$GX(t+1) = \begin{cases} (ub - lb) \times r_1 + lb, & rand < z \\ (r_2 - C) \times X_r(t) + D \times B, & rand \geq 0.5 \\ X(i) - D \times (D \times (X(t) - GX_r(t)) \\ \quad + r_3 \times (X(t) - GX_r(t))), & rand < 0.5 \end{cases}$$

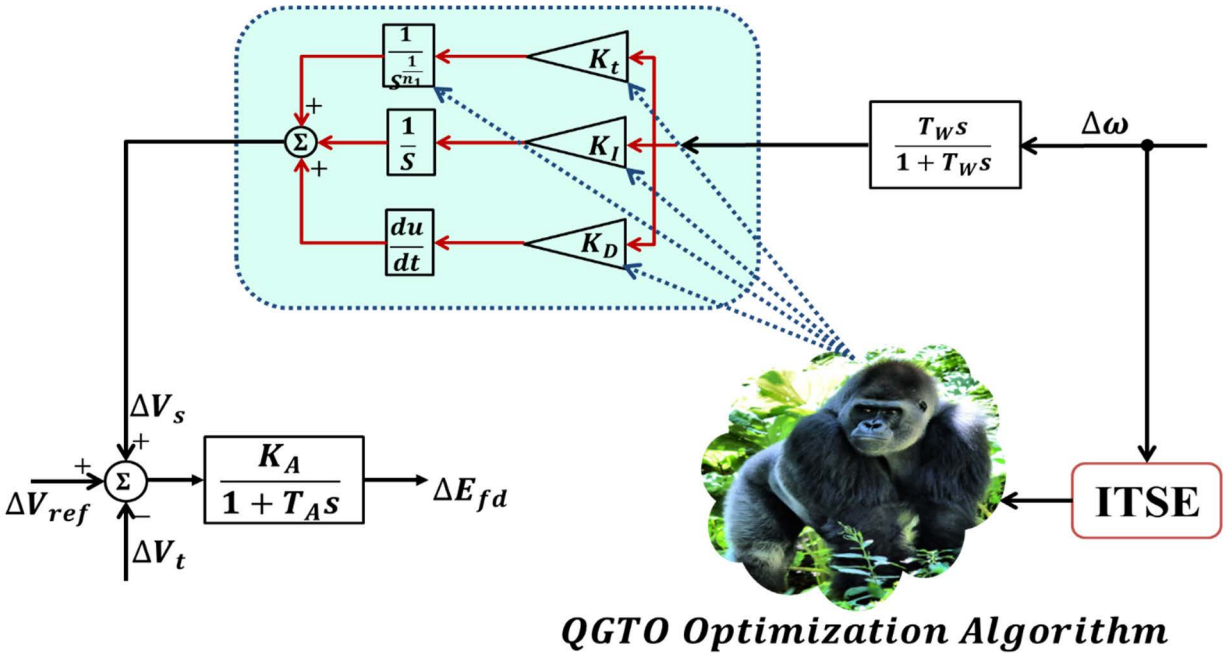

FIGURE 5. Block diagram of using QGTO for TID-based PSS optimum tuning.

$$C = (\cos(2\times r_4)+1)\times\left(1-\frac{it}{Maxit}\right)$$
$$D = C\times k$$
$$B = E\times X(t)$$
$$E = [-C, C] \tag{16}$$

where $GX(t+1)$ is the gorilla candidate position in the next iteration. lb and ub denote the lower and upper bounds of the variables, respectively. r_1, $rand$, r_2, r_3, and r_4 are random values ranging from 0 to 1. The z parameter has a range from 0 to 1. Also, $X(t)$ denotes the current vector of the gorilla position while $X_r(t)$ is a member of the gorillas randomly chosen from the entire gorillas and also $GX_r(t)$.The parameter k denotes a random value ranging from -1 to 1.

2) EXPLOITATION PHASE

During the exploitation phase, two strategies are applied. The first strategy is to follow the silverback, and it is applied when $C \geq W$, where W denotes a parameter to be set before the optimization operation. The first strategy can be mathematically evaluated as follows [47]:

$$GX(t+1) = D\times M\times(X(t)-X_{silverback})+X(t)$$
$$M = \left(\left|\frac{1}{N}\sum_{i=1}^{N}GX_i(t)\right|^{g}\right)^{\frac{1}{g}}$$
$$g = 2^D \tag{17}$$

where $X_{silverback}$ denotes the best solution, N is the total number of gorillas.

The second mechanism is the competition for adult females and it is applied when $C < W$. This mechanism is computed using the following equation:

$$GX(i) = X_{silverback} - (X_{silverback}\times Q - X(t)\times Q)\times A$$
$$Q = 2\times r_5 - 1$$
$$A = \beta\times H$$
$$H = \begin{cases} N_1, & rand \geq 0.5 \\ N_2, & rand < 0.5 \end{cases} \tag{18}$$

where β is a parameter to be given value before the optimization operation. r_5 is a random value ranging from 0 to 1.

B. THE PROPOSED QUANTUM ARTIFICIAL GORILLA TROOPS OPTIMIZER (QGTO)

In this subsection, quantum mechanics is used to develop the original GTO technique. This quantum model of a GTO technique is named the QGTO algorithm. Quantum Algorithm (QA) was firstly proposed in [49]. It was declared that QA could solve many difficulties based on the concepts and principles of quantum theory, including superposition of quantum states, entanglement, and intervention. Quantum-Inspired Evolutionary Algorithm (QEA) is one of the developing algorithms which was inspired by the concept of quantum computing [50]. This algorithm was successfully applied to solve several combinational optimization problems. The good performance of the QEA algorithm for finding a global best solution in a short time has attracted the attention of researchers to use quantum computing to develop algorithms such as quantum genetic algorithm (QGA) [51], multiscale quantum harmonic oscillator algorithm (MQHOA) [52], quantum Runge Kutta algorithm (QRUN) [53], quantum salp swarm algorithm (QSSA) [54], quantum chaos game

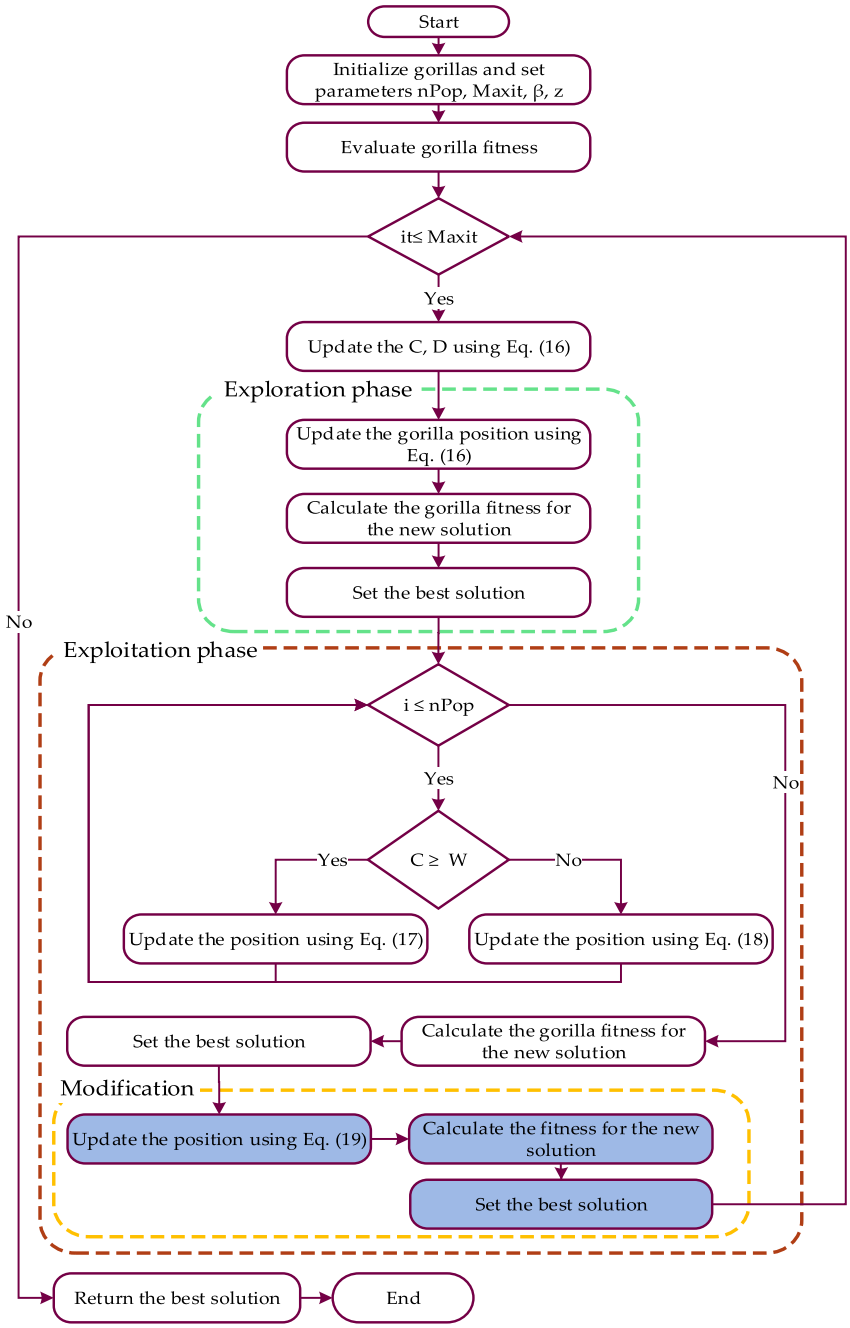

FIGURE 6. Flowchart of the proposed QGTO algorithm.

optimizer (QCGO) [55], and Quantum Henry gas solubility optimization algorithm (QHGSO) [56]. Quantum mechanics were employed to improve the PSO algorithm in [57]. In the quantum model, by employing the Monte Carlo method, the solution x_{new} is calculated as follows:

$$p = \frac{c_1 \times w \times X(t) + c_2 \times (1-w) \times X_{silverback}}{c_1 + c_2}$$

if $h \geq 0.5$

$$GX(t+1) = p + \alpha . |Mbest_i - X(t)| . \ln(1/u)$$

else

$$GX(t+1) = p - \alpha . |Mbest_i - X(t)| . \ln(1/u)$$

end (19)

where α is a design parameter, u and w represent uniform probability distribution in the range [0,1], and h is the random value ranging from 0 to 1. Mbest is the mean best of the population, and it is defined as the mean of the $X_{silverback}$ positions. It is calculated from this equation:

$$Mbest = \frac{1}{N} \sum_{i=1}^{N} X_i(t) \quad (20)$$

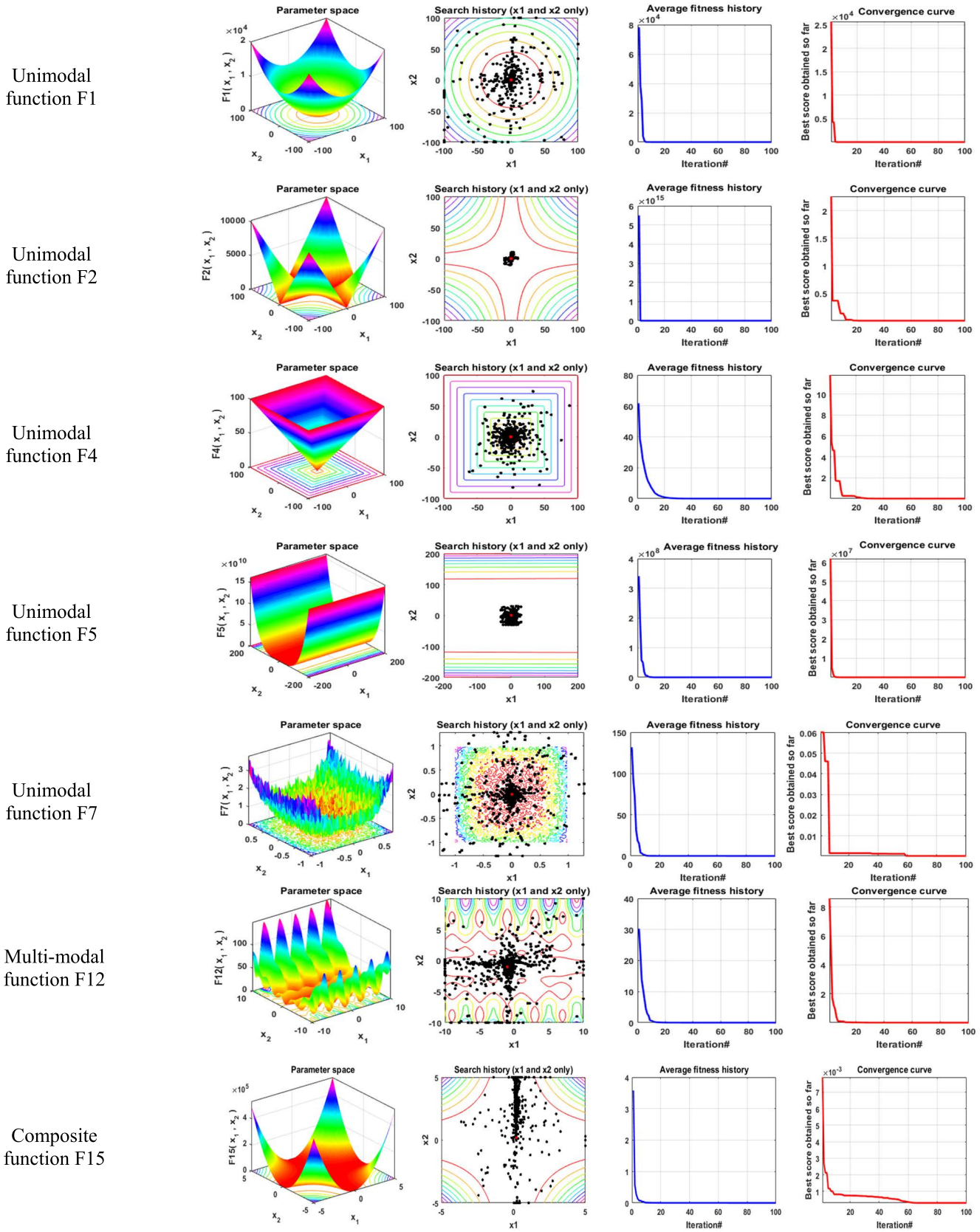

FIGURE 7. Qualitative metrics of nine benchmark functions: 2D views of the functions, search history, average fitness history, and convergence curve using the QGTO algorithm.

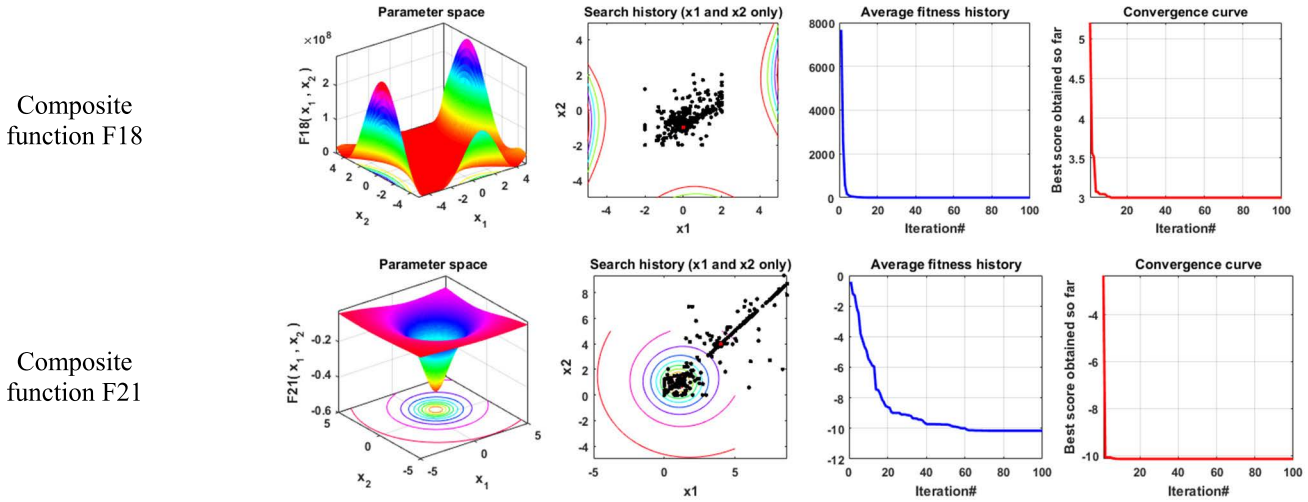

FIGURE 7. *(Continued.)* **Qualitative metrics of nine benchmark functions: 2D views of the functions, search history, average fitness history, and convergence curve using the QGTO algorithm.**

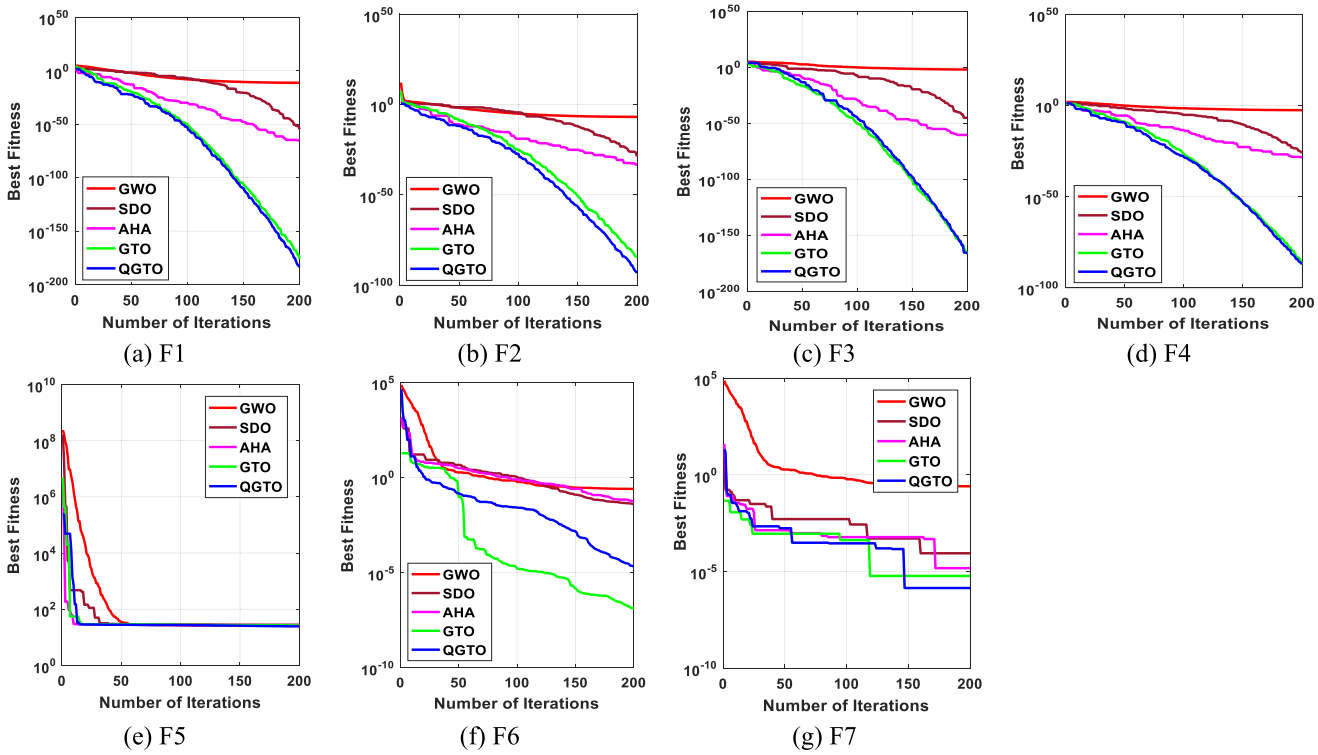

FIGURE 8. **The convergence curves of all algorithms for seven unimodal benchmark functions.**

The flow chart of the proposed QGTO technique is shown in Figure 6.

IV. SIMULATION OUTCOMES

This section will highlight the capability of the proposed optimization algorithm (QGTO) for reaching the optimum destination. This can be attained in two ways. Validation with the well-known benchmark functions is the first one and later is an important power system stability problem (i.e., low-frequency oscillations damping using PSS).

A. THE PROPOSED QGTO TECHNIQUE's PERFORMANCE

The effectiveness and performance of the QGTO algorithm are assessed on several benchmark functions in this subsection, including the minimum values, mean values, median values, maximum values, and standard deviation (STD) for

TABLE 1. The statistical results of unimodal benchmark functions using the proposed QGTO algorithm and other techniques.

Function		QGTO	GTO	AHA	SDO	GWO
F1	Best	**2.3E-184**	1.3E-176	3.01E-66	1.39E-55	4.47E-12
	Mean	**1.3E-171**	9.1E-152	3.87E-53	1.37E-51	3.12E-11
	Median	**3.3E-176**	4.2E-170	3.32E-59	3.74E-54	2.46E-11
	Worst	**1.5E-170**	1.8E-150	7.66E-52	8.43E-51	8.73E-11
	std	**0.00**	4.1E-151	1.71E-52	2.74E-51	2.31E-11
F2	Best	**5.75E-94**	2.96E-85	4.74E-34	1.83E-29	1.42E-07
	Mean	**2.23E-88**	1.44E-80	1.07E-29	3.76E-25	2.77E-07
	Median	**1.49E-90**	5.06E-82	3.11E-31	1.13E-26	2.66E-07
	Worst	**2.87E-87**	9.29E-80	9.48E-29	3.98E-24	4.78E-07
	std	**6.6E-88**	2.93E-80	2.51E-29	9.1E-25	9.9E-08
F3	Best	6.1E-167	**3.8E-167**	3.15E-61	6.27E-46	0.008462
	Mean	4.8E-143	**3.9E-149**	4.36E-48	6.91E-34	0.610441
	Median	7.7E-153	**9.3E-157**	1.01E-54	1.4E-39	0.185412
	Worst	9.6E-142	**7.4E-148**	6.68E-47	1.38E-32	3.567009
	std	2.1E-142	**1.7E-148**	1.53E-47	3.09E-33	0.827115
F4	Best	1.09E-87	**8.11E-88**	5.07E-29	1.11E-26	0.002608
	Mean	**2.32E-82**	1.3E-80	4.63E-26	4.52E-23	0.008
	Median	**2.01E-85**	8.8E-83	1.05E-27	1.14E-23	0.007092
	Worst	**3.3E-81**	1.37E-79	4.23E-25	1.94E-22	0.016667
	std	**7.52E-82**	3.51E-80	1.02E-25	6.34E-23	0.003845
F5	Best	**24.44049**	25.98586	26.40974	27.90967	25.92515
	Mean	**25.35535**	26.1865	27.5024	28.65096	27.18903
	Median	**25.10151**	26.18963	27.47815	28.74726	27.09814
	Worst	26.68861	**26.44787**	28.53304	28.98699	28.79035
	std	0.660082	**0.119778**	0.472237	0.295026	0.72182
F6	Best	2.14E-05	**1.28E-07**	0.058638	0.039957	0.252254
	Mean	0.00021	**0.000152**	0.442296	2.568541	0.647554
	Median	0.000123	**2.01E-05**	0.393054	2.038779	0.611378
	Worst	0.000754	**0.001805**	1.029767	7.250251	1.172757
	std	**0.000204**	0.0004	0.249876	1.852701	0.280888
F7	Best	**1.38E-06**	5.83E-06	1.47E-05	8.66E-05	0.001477
	Mean	**0.000116**	0.000168	0.000346	0.002356	0.004433
	Median	**0.000102**	0.000152	0.000219	0.001136	0.003685
	Worst	**0.000343**	0.000421	0.001202	0.013813	0.01033
	std	**8.85E-05**	0.00012	0.000292	0.003331	0.002554

The best-obtained values are in bold.

the solutions attained by the proposed QGTO algorithm, the original GTO algorithm and the three recent optimization algorithms, including the artificial hummingbird algorithm (AHA) [58], supply-demand-based optimization (SDO) algorithm [59], and grey wolf optimizer (GWO) [60]. The results of the QGTO algorithm are compared with these well-known optimization algorithms. These techniques have been performed for the maximum number of iterations is 200, the population size is 50, and 20 independent runs using MATLAB R2016a. All simulations have been implemented on a laptop, including Core i5-4210U CPU@ 2.40 GHz of speed and 8 GB of RAM. The Qualitative metrics using the QGTO algorithm for nine benchmark functions, including 2D views of the functions, search history, average fitness history, and convergence curve, are illustrated in Figure 7.

The proposed QGTO algorithm and other techniques are applied for three benchmark functions (unimodal, multi-modal, and composite benchmark functions) to assess the performance of the QGTO algorithm in comparison with four recent algorithms including original GTO, AHA, SDO, and GWO algorithms. The optimal values were achieved with these algorithms shown in bold. The performance of the unimodal benchmark functions is given in Table 1. In unimodal benchmark functions, the proposed QGTO algorithm found the optimal solution in the functions F1, F2, F4, F5, and F7. The original GTO algorithm was only best in the F3 and F6. In this category of benchmark functions, since there is only one global optimum, the performance of the relevant algorithms is evaluated during the exploitation phase. Based on the results, the performance of the proposed QGTO

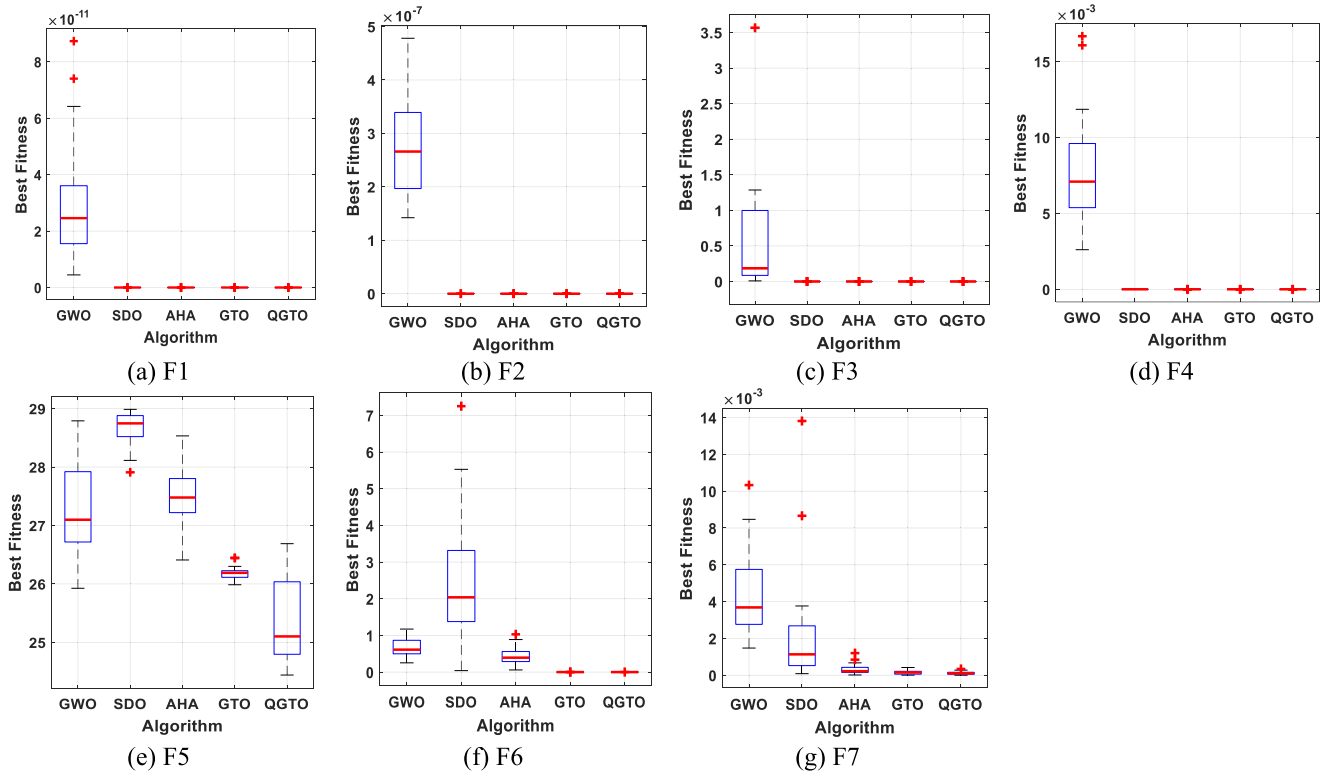

FIGURE 9. Boxplots for all algorithms for seven unimodal benchmark functions.

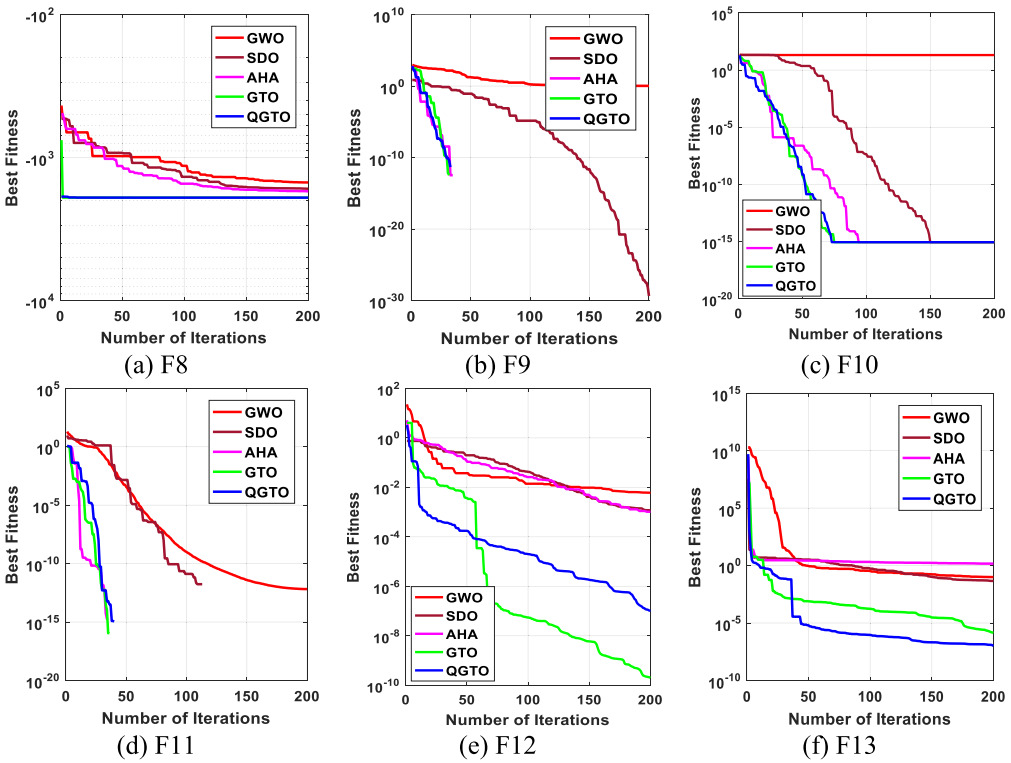

FIGURE 10. The convergence curves of all algorithms for six multi-modal benchmark functions.

algorithm is seen to be superior in the related functions, so it is observed to be fast and successful in the exploitation phase.

In Tables 2 and 3, the results of the multi-modal and multi-modal, and composite functions are given. The multi-modal

TABLE 2. The statistical results of multi-modal benchmark functions using the proposed technique and other algorithms.

Function		QGTO	GTO	AHA	SDO	GWO
	Best	**-1909.05**	**-1909.05**	-1724.06	-1655	-1495.31
	Mean	-1895.79	**-1909.05**	-1551.13	-1312.83	-1245.57
F8	Median	**-1909.05**	**-1909.05**	-1562.44	-1385.86	-1224.18
	Worst	-1823.3	**-1909.05**	-1364.15	-598.802	-1123.85
	Std	24.92127	**0.000616**	93.45685	294.008	104.0153
	Best	**0.00**	**0.00**	**0.00**	4.33E-30	1.062467
	Mean	**0.00**	**0.00**	**0.00**	1.75E-22	9.801018
F9	Median	**0.00**	**0.00**	**0.00**	4.17E-25	9.824713
	Worst	**0.00**	**0.00**	**0.00**	3.02E-21	24.96968
	Std	**0.00**	**0.00**	**0.00**	6.75E-22	5.565812
	Best	**8.88E-16**	**8.88E-16**	**8.88E-16**	**8.88E-16**	20.76487
	Mean	**8.88E-16**	**8.88E-16**	**8.88E-16**	**8.88E-16**	20.92344
F10	Median	**8.88E-16**	**8.88E-16**	**8.88E-16**	**8.88E-16**	20.94465
	Worst	**8.88E-16**	**8.88E-16**	**8.88E-16**	**8.88E-16**	21.06309
	Std	**0.00**	**0.00**	**0.00**	**0.00**	0.083433
	Best	**0.00**	**0.00**	**0.00**	**0.00**	6.56E-13
	Mean	**0.00**	**0.00**	**0.00**	**0.00**	0.009891
F11	Median	**0.00**	**0.00**	**0.00**	**0.00**	4.55E-12
	Worst	**0.00**	**0.00**	**0.00**	**0.00**	0.055407
	Std	**0.00**	**0.00**	**0.00**	**0.00**	0.015766
	Best	1.03E-07	**2.01E-10**	0.001029	0.001152	0.006066
	Mean	1.08E-05	**6.7E-07**	0.008654	0.23467	0.026151
F12	Median	5.93E-06	**7.98E-08**	0.006918	0.067805	0.023474
	Worst	4.18E-05	**4.23E-06**	0.031416	1.492821	0.047176
	Std	1.15E-05	**1.09E-06**	0.007552	0.352063	0.013414
	Best	**1.02E-07**	1.42E-06	1.456302	0.046216	0.09955
	Mean	**2.3E-05**	0.005645	2.339115	1.867552	0.613832
F13	Median	**3.3E-06**	0.000236	2.436057	1.934246	0.609981
	Worst	**0.000186**	0.044505	2.969591	2.999924	1.044
	std	**4.66E-05**	0.010476	0.361111	0.961284	0.280029

The best-obtained values are in bold.

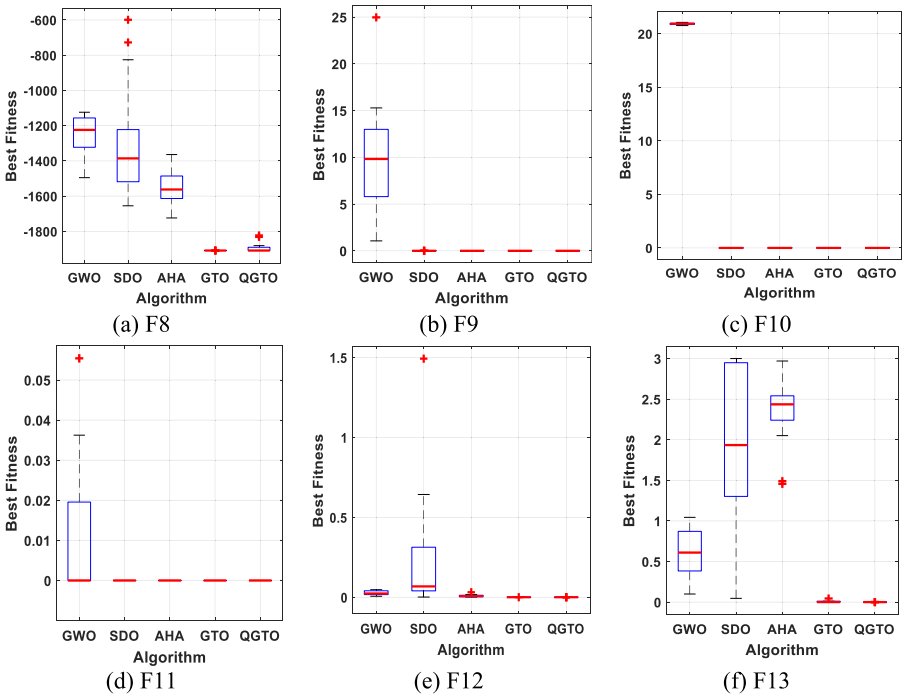

FIGURE 11. Boxplots for all algorithms for multi-modal benchmark functions.

TABLE 3. The statistical results of composite benchmark functions using the proposed technique and other well-known algorithms.

Function		QGTO	GTO	AHA	SDO	GWO
	Best	**0.998004**	**0.998004**	**0.998004**	**0.998004**	**0.998004**
	Mean	**0.998004**	**0.998004**	**0.998004**	3.494696	3.892106
F14	Median	**0.998004**	**0.998004**	**0.998004**	1.495017	2.982105
	Worst	**0.998004**	**0.998004**	**0.998004**	12.67051	12.67051
	std	1.61E-16	**8.82E-17**	1.03E-09	3.953203	3.727681
	Best	**0.000307**	**0.000307**	**0.000307**	**0.000307**	0.00031
	Mean	0.000353	0.000399	**0.000318**	0.00067	0.003547
F15	Median	**0.000307**	**0.000307**	0.000308	0.000527	0.000546
	Worst	0.001223	0.001223	**0.000485**	0.002121	0.020363
	std	0.000205	0.000282	**3.95E-05**	0.000473	0.007255
	Best	**-1.03163**	**-1.03163**	**-1.03163**	**-1.03163**	**-1.03163**
	Mean	**-1.03163**	**-1.03163**	**-1.03163**	-1.03005	-1.03158
F16	Median	**-1.03163**	**-1.03163**	**-1.03163**	**-1.03163**	**-1.03163**
	Worst	**-1.03163**	**-1.03163**	**-1.03163**	-1.00046	-1.03063
	std	1.76E-16	**1.69E-16**	1.18E-12	0.006966	0.000223
	Best	**0.397887**	**0.397887**	**0.397887**	**0.397887**	0.397888
	Mean	**0.397887**	**0.397887**	**0.397887**	**0.397987**	0.397891
F17	Median	**0.397887**	**0.397887**	**0.397887**	**0.397887**	0.397891
	Worst	**0.397887**	**0.397887**	**0.397887**	0.399795	0.397897
	std	**0.00**	**0.00**	**0.00**	0.000426	3.01E-06
	Best	**3.00**	**3.00**	**3.00**	**3.00**	**3.00**
	Mean	**3.00**	**3.00**	**3.00**	4.371758	3.000068
F18	Median	**3.00**	**3.00**	**3.00**	**3.00**	3.000036
	Worst	**3.00**	**3.00**	**3.00**	30.41145	3.000238
	std	**1.24E-15**	1.5E-15	1.6E-15	6.129111	6.53E-05
	Best	**-0.30048**	**-0.30048**	**-0.30048**	**-0.30048**	**-0.30048**
	Mean	**-0.30048**	**-0.30048**	-0.30047	-0.2893	**-0.30048**
F19	Median	**-0.30048**	**-0.30048**	-0.30047	-0.30038	**-0.30048**
	Worst	**-0.30048**	**-0.30048**	-0.30044	-0.19165	**-0.30048**
	std	**1.14E-16**	**1.14E-16**	1.04E-05	0.026531	**1.14E-16**
	Best	**-3.322**	**-3.322**	**-3.322**	**-3.322**	-3.32198
	Mean	**-3.322**	-3.29822	-3.30415	-3.09697	-3.22876
F20	Median	**-3.322**	**-3.322**	**-3.322**	-3.2031	-3.26239
	Worst	**-3.322**	-3.2031	-3.2031	-0.89904	-2.84039
	std	**3.81E-16**	0.048793	0.043552	0.550986	0.125558
	Best	**-10.1532**	**-10.1532**	**-10.1532**	**-10.1532**	-10.1502
	Mean	**-10.1532**	**-10.1532**	-10.1059	-8.703	-8.51218
F21	Median	**-10.1532**	**-10.1532**	-10.153	**-10.1532**	-10.1413
	Worst	**-10.1532**	**-10.1532**	-9.2237	-4.99677	-2.62918
	std	**2.31E-15**	2.41E-15	0.207648	2.23952	2.963153
	Best	**-10.4029**	**-10.4029**	**-10.4029**	**-10.4029**	-10.4024
	Mean	**-10.4029**	**-10.4029**	-10.0864	-8.45822	-10.0134
F22	Median	**-10.4029**	**-10.4029**	**-10.4029**	**-10.4029**	-10.3959
	Worst	**-10.4029**	**-10.4029**	-5.08767	-1.0677	-2.76526
	std	3.97E-15	**3.8E-15**	1.19136	3.128689	1.706042
	Best	**-10.5364**	**-10.5364**	**-10.5364**	**-10.5364**	-10.5348
	Mean	**-10.5364**	**-10.5364**	-10.2621	-7.90449	-9.74305
F23	Median	**-10.5364**	**-10.5364**	**-10.5364**	-10.5357	-10.5274
	Worst	**-10.5364**	**-10.5364**	-5.12848	-3.79083	-2.42135
	std	**2.41E-15**	**2.41E-15**	1.208388	3.015319	2.418464

The best-obtained values are in bold.

functions have multiple local minima and one global optimum. These functions can be a very important roadmap for assessing exploration and exploitation phases. Table 2 tabulated the simulation results of each algorithm over F8

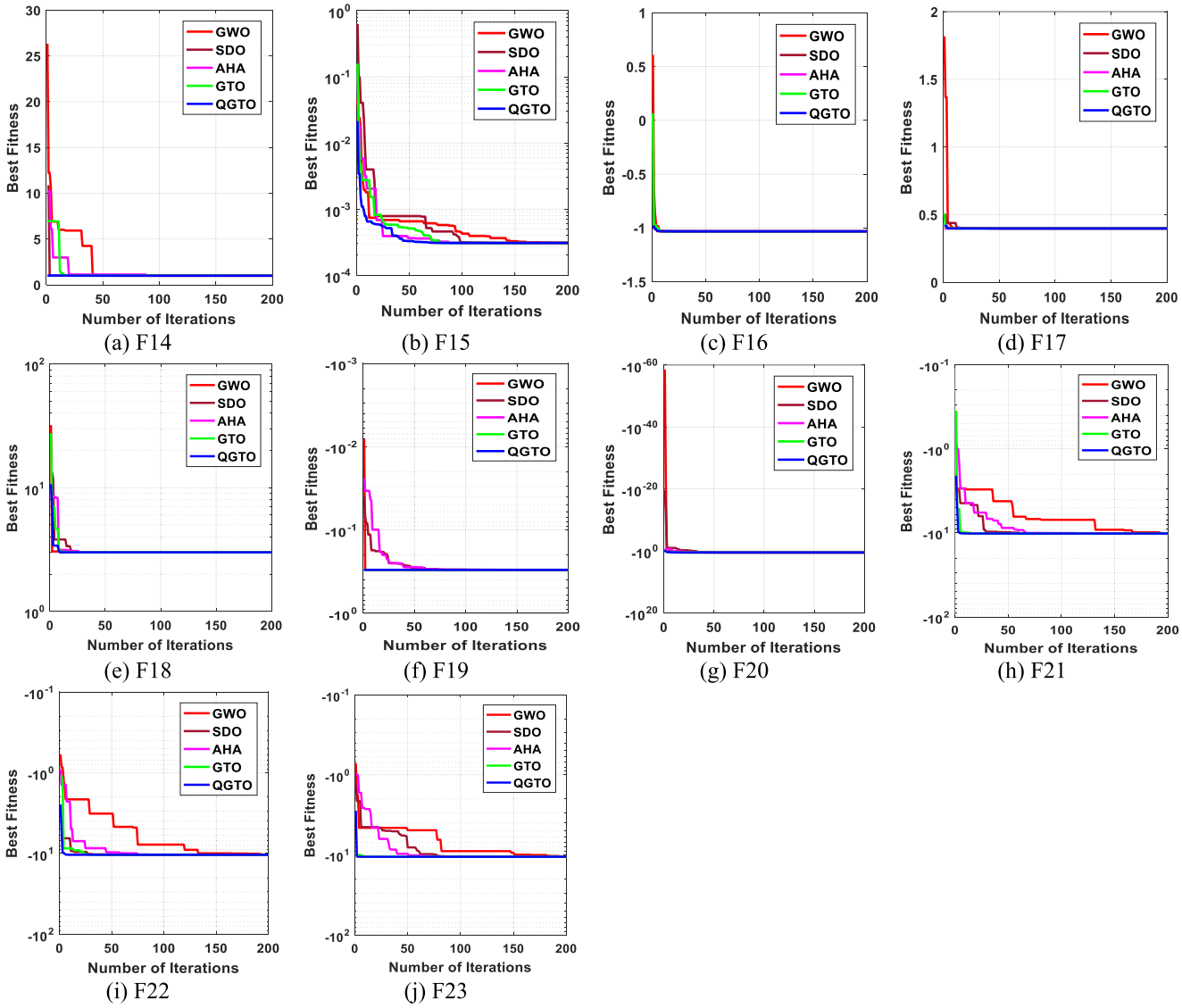

FIGURE 12. The convergence curves of all algorithms for composite benchmark functions.

TABLE 4. Optimum parameters of DIPSS using GTO and QGTO.

QGTO						
Cost function	K_{s1}	K_{s2}	T_{d1}	T_{d2}	T_{d3}	T_{d4}
1.5951e-05	-5.1144	48.9266	0.1294	0.0271	0.0100	0.9083
GTO						
2.7229e-05	-5.0000	5.0000	0.4752	0.0543	1.4028	0.0728

to F13 functions. The proposed QGTO technique reaches the best solution in the F8, F9, F10, F11, and F13. The original GTO algorithm found the better solution in F12. Based on the results of the multi-modal functions, it has been determined that the proposed QGTO algorithm has a better performance compared to the others. Similarly, Table 3 presents the statistical results for the functions F14 to F23. The composite function evaluates the exploration of the optimization technique. The QGTO technique achieves the best solution for all functions F14 to F23. In these functions, the proposed QGTO algorithm is the best optimizer compared to others. That indicates the QGTO technique's efficient performance in the exploration phases. Figure 8 displays the convergence curves of all these algorithms for the unimodal

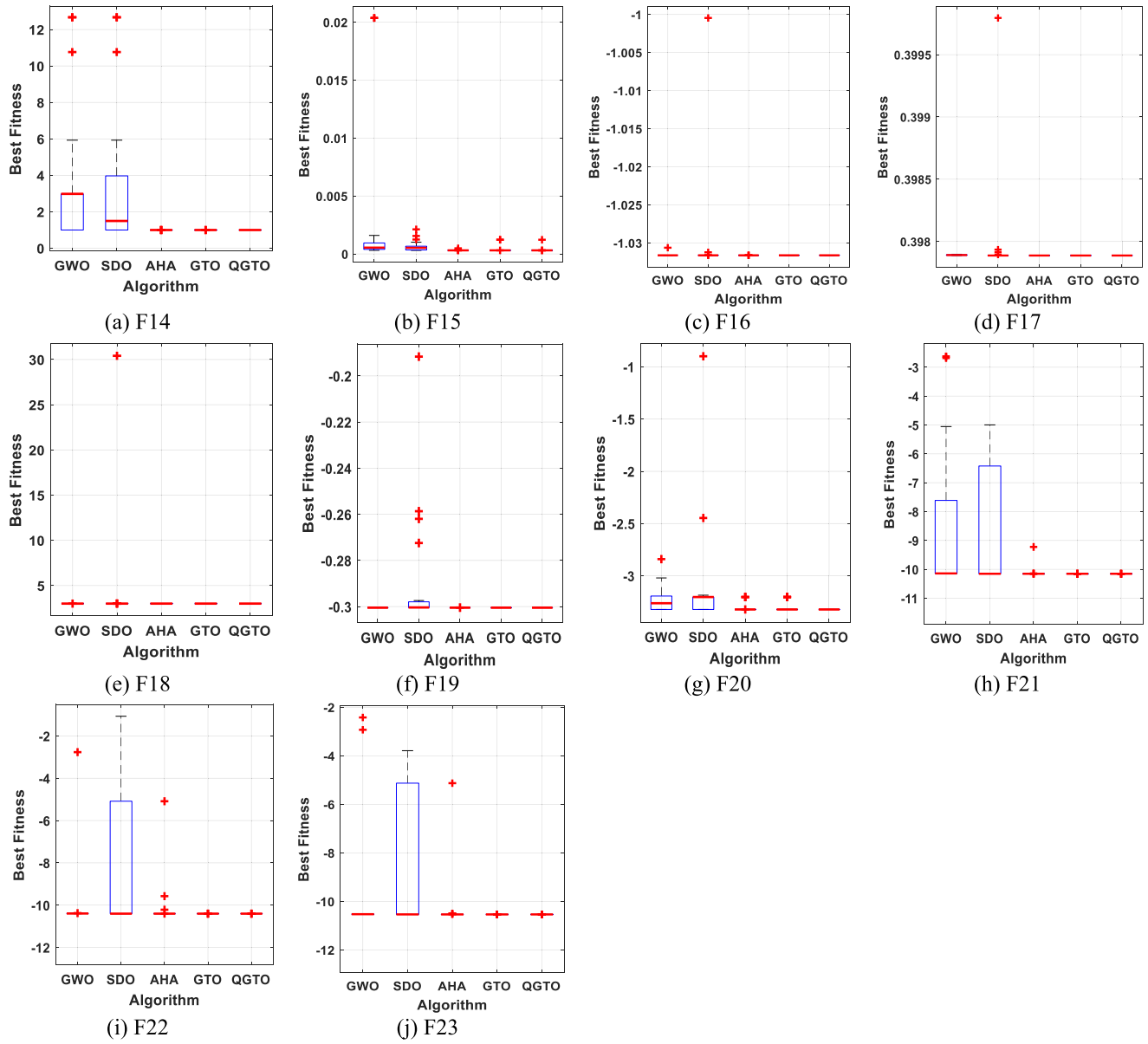

FIGURE 13. Boxplots for all algorithms for composite benchmark functions.

TABLE 5. Optimal parameters of TID-PSS using various optimization algorithms.

Param. \ optimizer	RUN	AEO	GBO	GTO	QGTO
K_t	42.1642	43.6415	42.5394	34.7803	42.5176
K_i	3.03322	3.85309	3.6898	1.8560	3.70098
K_d	6.51716	6.59219	6.4500	6.0306	6.49703
n	18.1634	47.8622	44.4448	20.0620	42.0236
Cost (ITAE)	4.8723e-06	4.7877e-06	4.7893e-06	4.993e-06	4.7865e-06

benchmark function, while Figure 9 displays the Boxplots for these algorithms for this type of function. Also, the convergence curves of these algorithms for the multi-modal benchmark functions are presented in Figure 10, while the Boxplots for each algorithm for these functions are illustrated in Figure 11. Finally, Figure 12 shows the convergence curves of all techniques for the composite benchmark functions, while Figure 13 illustrates the Boxplots for all algorithms for

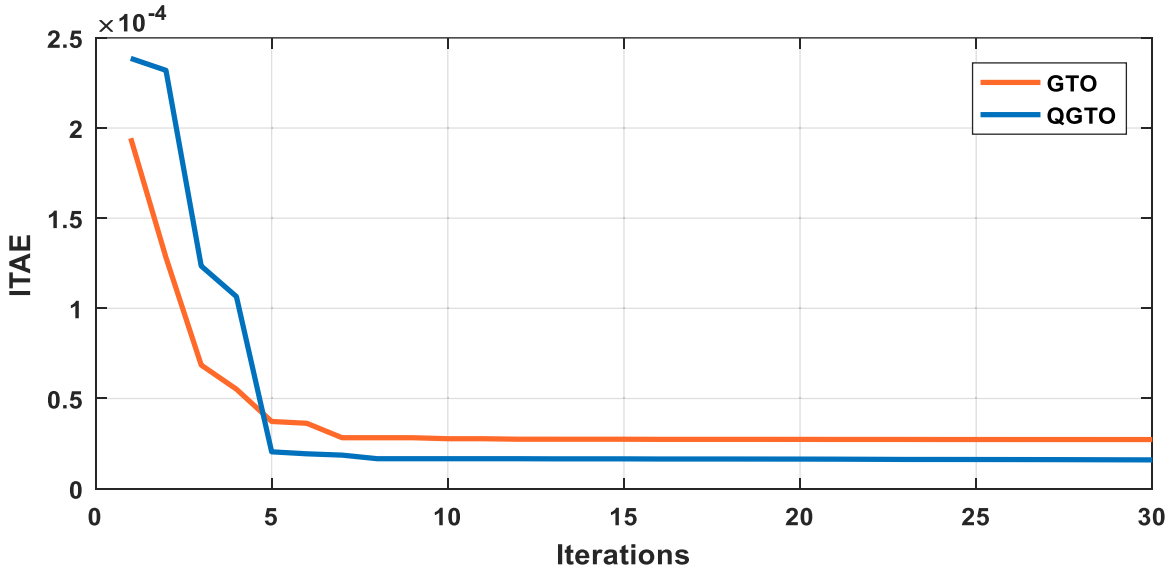

FIGURE 14. Convergence curves of GTO and QGTO employed for optimum parameters estimation of the DIPSS.

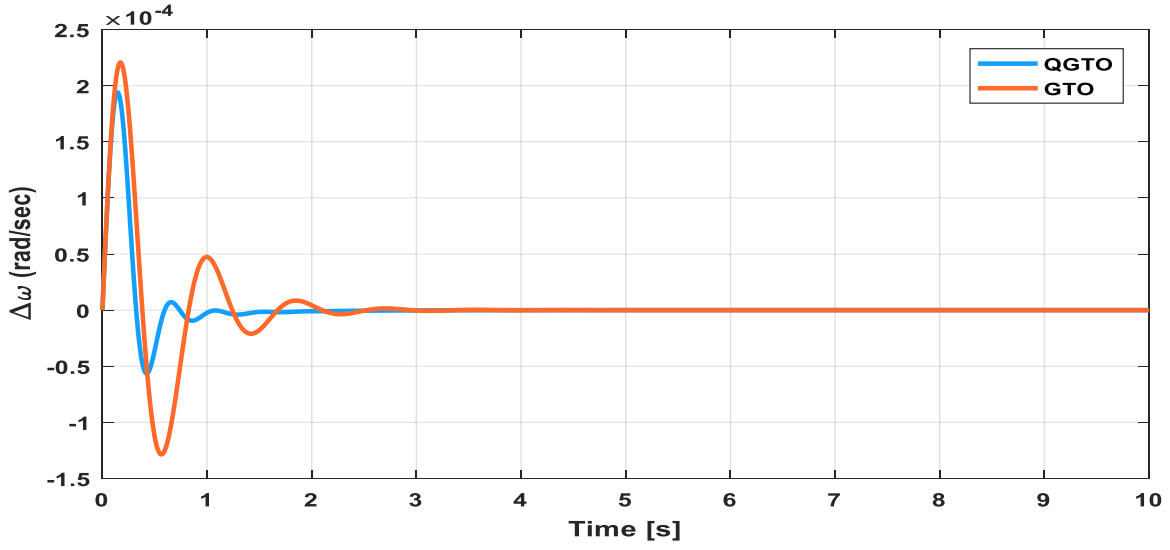

FIGURE 15. Change in rotor speed in case of using DIPSS.

this type of benchmark function. From these figures, it is seen that the proposed QGTO technique achieves a stable point for all functions and the boxplots of the QGTO algorithm are very narrow for most functions compared to the other algorithms.

B. REAL-LIFE APPLICABILITY

Upon demonstrating the superiority of QGTO through the well-known benchmark functions, this section spots light on its applicability of it in one of the electrical power systems applications. Assessment of the effectiveness of QGTO to optimally tune investigated PSS parameters will be achieved with the help of SMIB embedded with PSS. The SMIB model data can be attained from [20]. The system response will be studied while there is a change of 0.1 p.u in T_m. The simulation is carried out with the help of an Intel core TM i7- 4790 CPU, 8 GB RAM laptop using the MATLAB 2020a platform.

The employed evaluation will be achieved through three stages. First, the GTO and QGTO will be used to attain the optimal parameters of the DIPSS. After that, the QGTO will be used for the optimum parameter tuning of TID-PSS. The obtained results will be compared with the CPSS and DIPSS. Finally, the investigation of QGTO to reach the optimum parameters of FOPID-PSS will be applied. All the obtained results will be compared to take a full picture of the performance of investigated PSSs.

In the case of employing the DIPSS, the QGTO shows fast convergence and lower fitness function over the course of

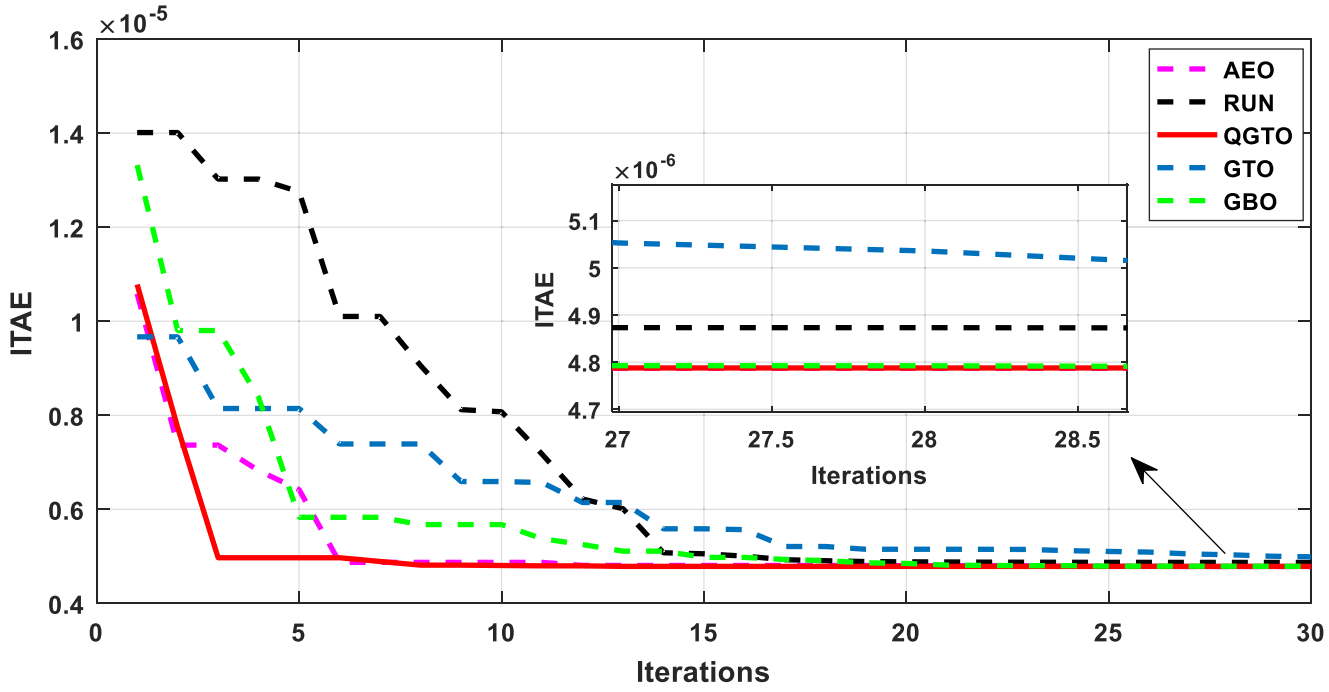

FIGURE 16. Convergence curves for optimum tuning of the TID-PSS with various optimizers.

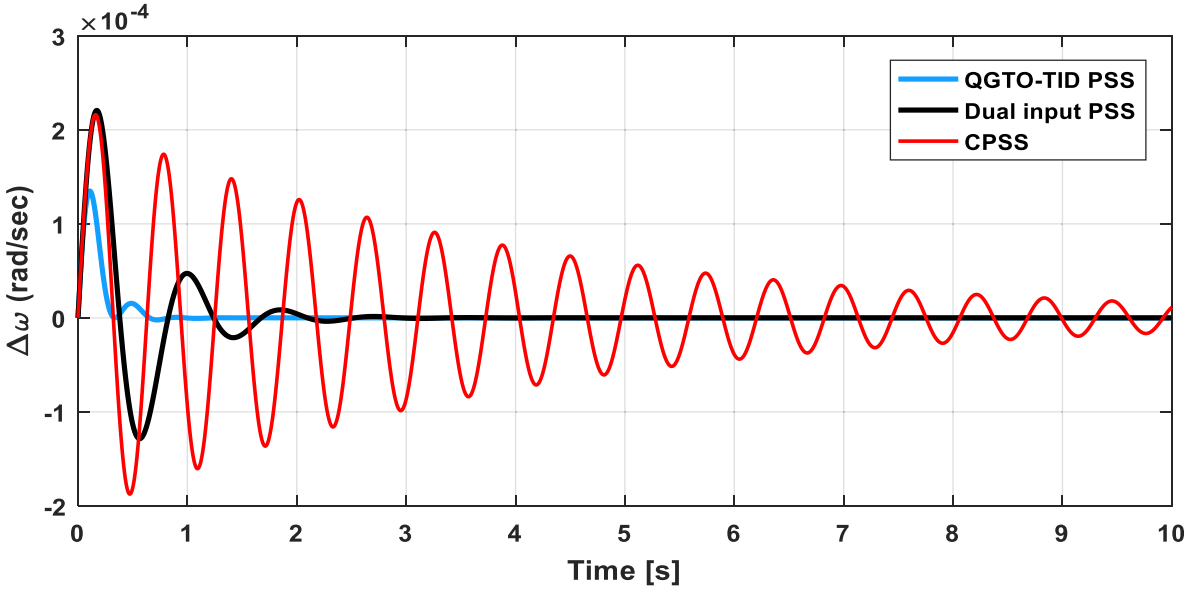

FIGURE 17. Change in rotor speed in case of using QGTO-TID PSS.

iterations, as illustrated in Figure 14. Also, from Figure 15, it can be proven that the maximum overshot (MOS) of change in rotor speed signal in the case of QGTO is lower than its value while using GTO. The optimized parameters of DIPSS, as well as the attained cost functions, are tabulated in Table 4.

On the other hand, the QGTO ensures superior performance over the Artificial ecosystem-based optimization (AEO), RUN, GTO, and Gradient-based optimization (GBO) optimization algorithms, as shown in Figure 16. It reaches the lowest ITAE value of (4.7877e-06), while the GTO reaches the highest value of (4.993e-06), which can be obtained from Table 5.

Figure 17 shows the effect of using the CPSS, DIPSS, and QGTO optimized TID- PSS. There is no doubt that the QGTO optimized TID- PSS shows better performance over the other

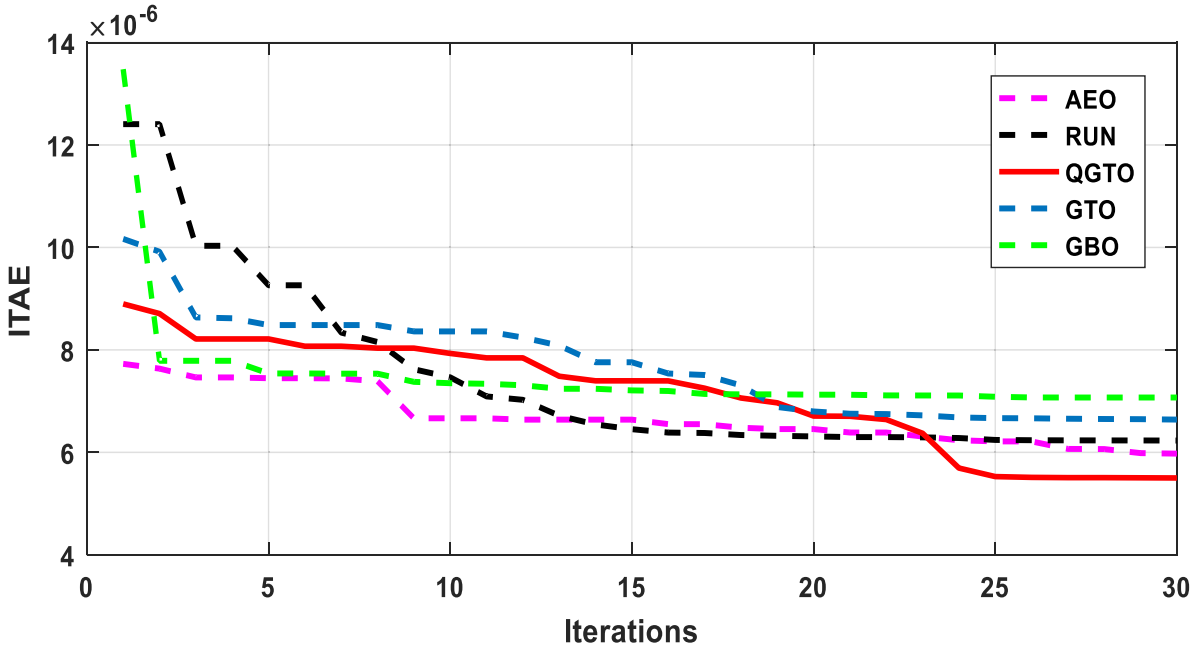

FIGURE 18. Convergence curves for optimum tuning of FOPID-PSS with various optimizers.

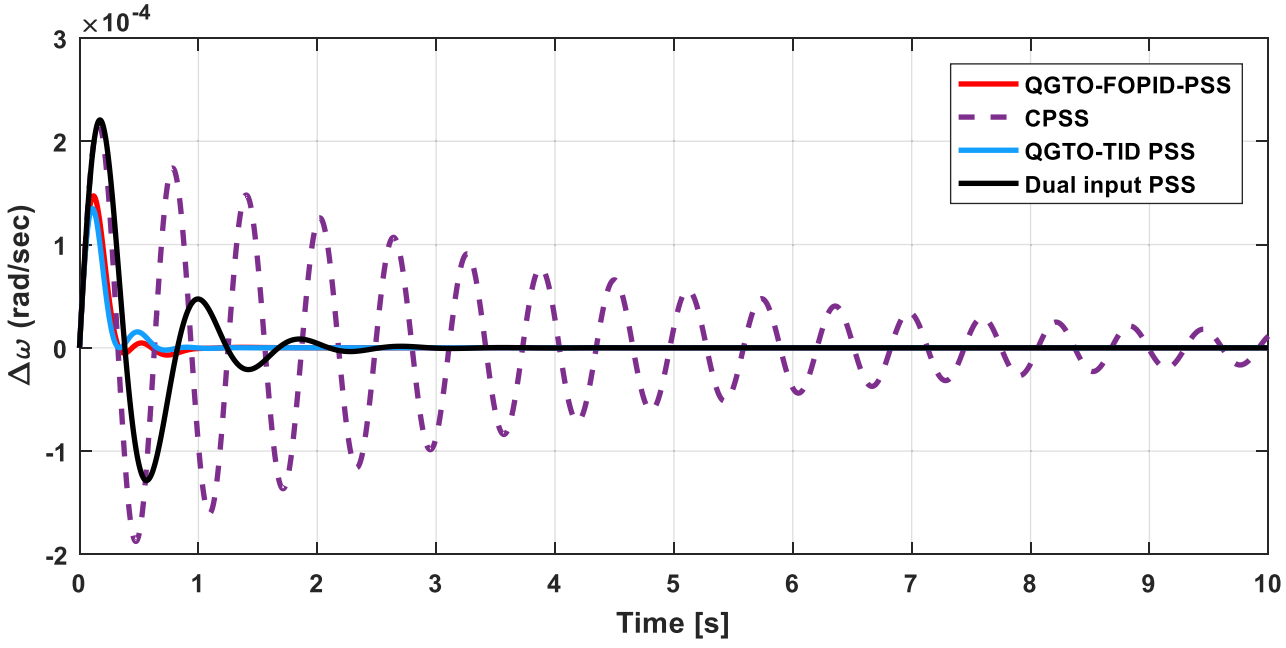

FIGURE 19. Change in rotor speed in case of using QGTO-FOPID PSS.

PSSs. This can be clarified from the lowest MOS, MUS, and lower settling time.

As one of the fractional-order controller families, the capability of the QGTO for the optimum tuning of FOPID-PSS is also employed. Also, the QGTO convergence characteristics show fast convergence and lower ITAE over the AEO, RUN, GTO, and GBO algorithms which are shown in Figure 18 and tabulated in Table 6.

A complete evaluation of the obtained results using QGTO for the CPSS, DIPSS, FOPID-PSS, and TID-PSS.

TABLE 6. Optimal parameters of FOPID-PSS using various optimization algorithms.

Param. \ optimizer	RUN	AEO	GBO	GTO	QGTO
K_P	14.7256	14.6563	14.8356	15.0000	14.9760
K_i	8.4505	13.7664	2.82556	5.1692	15.0000
K_d	6.07173	6.73125	7.01909	6.2823	5.6431
λ	0.162265	0.183128	0.503684	0.3085	0.1058
μ	0.944647	0.942915	0.876681	0.9108	1.0000
ITAE	6.2303e-06	5.975e-06	7.0704e-06	6.6394e-06	5.4999e-06

The TID-PSS has better performance indices in terms of lowest MOS, MUS, and settling time overall compatible structures of PSS, as can be proven in Figure 19.

V. CONCLUSION

Aberration in the electrical power system can have a range of detrimental effects on its stability. Hence, maintaining its stability in such operational conditions has become a constant issue for power engineers. Power system stabilizers (PSSs) are one of the proposed solutions that are designed to act as auxiliary controllers in order to address the instability difficulties caused by disturbances. This research manuscript proposes a comprehensive evaluation of optimal parameters tuning of different PSSs using a novel Quantum Artificial Gorilla Troops Optimizer. Validation of the proposed algorithm is proofed using the well-known benchmark functions. The novel proposed optimization algorithm shows superiority over the gorilla troops optimizer and compatible optimization algorithms. Moreover, four different structures of PSS, namely dual input PSS (DIPSS), Tilt-integral-derivative (TID-PSS), fractional-order proportional-integral-derivative (FOPID-PSS), and the conventional lead-lag PSS are employed for the comprehensive investigation of proposed algorithm performance and optimum tuning capability. With the utilization of the proposed algorithm, the fitness function of TID-PSS has the lowest value of 0.000004993 compared to DIPSS and FOPID-PSS, which reach 0.000027229 and 0.0000066394, respectively. Moreover, the TID-PSS has superior performance indices in terms of lowest maximum overshoot, maximum undershoot, and lower settling time. This research will be extended to include sensitivity analysis as future work. This analysis will prove the capability of the proposed PSS structure.

REFERENCES

[1] A. A. Sallam and O. P. Malik, *Power System Stability: Modelling, Analysis and Control*, 1st ed. London, U.K.: The Institution of Engineering and Technology, 2015.

[2] P. Kundur, N. J. Balu, and M. G. Lauby, *Power System Stability and Control*. New York, NY, USA: McGraw-Hill, 1994.

[3] *IEEE Recommended Practice for Excitation System Models for Power System Stability Studies*, PES, Tokyo, vol. 2005, Apr. 2006.

[4] S. Ekinci, "Optimal design of power system stabilizer using sine cosine algorithm," *J. Fac. Eng. Archit. Gazi Univ.*, vol. 34, no. 3, pp. 1329–1350, 2019, doi: 10.17341/gazimmfd.460529.

[5] X.-L. Huang, X. Ma, and F. Hu, "Editorial: Machine learning and intelligent communications," *Mobile Netw. Appl.*, vol. 23, no. 1, pp. 68–70, Feb. 2018, doi: 10.1007/s11036-017-0962-2.

[6] A. F. Mijbas, B. A. A. Hasan, and H. A. Salah, "Optimal stabilizer PID parameters tuned by chaotic particle swarm optimization for damping low frequency oscillations (LFO) for single machine infinite bus system (SMIB)," *J. Electr. Eng. Technol.*, vol. 15, no. 4, pp. 1577–1584, Jul. 2020, doi: 10.1007/s42835-020-00442-5.

[7] B. Dasu, M. Sivakumar, and R. Srinivasarao, "Interconnected multimachine power system stabilizer design using whale optimization algorithm," *Protection Control Modern Power Syst.*, vol. 4, no. 1, Dec. 2019, doi: 10.1186/s41601-019-0116-6.

[8] R. Devarapalli, B. Bhattacharyya, and A. Kumari, "Enhancing oscillation damping in a power network using EWOA technique," in *Advances in Smart Grid Automation and Industry* (Lecture Notes in Electrical Engineering), vol. 693. Singapore: Springer, 2021, pp. 27–36, doi: 10.1007/978-981-15-7675-1_3.

[9] R. Devarapalli, B. Bhattacharyya, V. Kumar, and S. Kumar, "Improved moth flame optimization in systematization of STATCOM and PSS," in *Advances in Smart Grid Automation and Industry* (Lecture Notes in Electrical Engineering), vol. 693. Singapore: Springer, 2021, pp. 481–491, doi: 10.1007/978-981-15-7675-1_48.

[10] R. Devarapalli, B. Bhattacharyya, and J. K. Saw, "Controller parameter tuning of a SMIB system with STATCOM using ALO algorithm for the power system stability improvement," *Adv. Control Appl. Eng. Ind. Syst.*, vol. 2, no. 3, p. e45, Jun. 2020, doi: 10.1002/adc2.45.

[11] S. Ekinci, D. Izci, H. L. Zeynelgil, and S. Orenc, "An application of slime mould algorithm for optimizing parameters of power system stabilizer," in *Proc. 4th Int. Symp. Multidisciplinary Stud. Innov. Technol. (ISMSIT)*, 2020, pp. 1–5, doi: 10.1109/ISMSIT50672.2020.9254597.

[12] T. Guesmi, B. M. Alshammari, Y. Almalaq, A. Alateeq, and K. Alqunun, "New coordinated tuning of SVC and PSSs in multimachine power system using coyote optimization algorithm," *Sustainability*, vol. 13, no. 6, p. 3131, Mar. 2021, doi: 10.3390/su13063131.

[13] S. Ekinci, D. Izci, and B. Hekimoglu, "Implementing the Henry gas solubility optimization algorithm for optimal power system stabilizer design," *Electrica*, vol. 21, no. 2, pp. 250–258, May 2021, doi: 10.5152/electrica.2021.20088.

[14] P. Dey, A. Bhattacharya, and P. Das, "Tuning of power system stabilizer for small signal stability improvement of interconnected power system," *Appl. Comput. Informat.*, vol. 16, nos. 1–2, pp. 3–28, Dec. 2017, doi: 10.1016/j.aci.2017.12.004.

[15] M. A. Abido, "Optimal design of power-system stabilizers using particle swarm optimization," *IEEE Trans. Energy Convers.*, vol. 17, no. 3, pp. 406–413, Sep. 2002, doi: 10.1109/TEC.2002.801992.

[16] D. Chitara, K. R. Niazi, A. Swarnkar, and N. Gupta, "Cuckoo search optimization algorithm for designing of a multimachine power system stabilizer," *IEEE Trans. Ind. Appl.*, vol. 54, no. 4, pp. 3056–3065, Jul./Aug. 2018, doi: 10.1109/TIA.2018.2811725.

[17] S. Ekinci and B. Hekimoglu, "Parameter optimization of power system stabilizer via salp swarm algorithm," in *Proc. 5th Int. Conf. Electr. Electron. Eng. (ICEEE)*, May 2018, pp. 143–147, doi: 10.1109/ICEEE2.2018.8391318.

[18] H. K. Abdulkhader, J. Jacob, and A. T. Mathew, "Fractional-order lead-lag compensator-based multi-band power system stabiliser design using a hybrid dynamic GA-PSO algorithm," *IET Gener., Transmiss. Distrib.*, vol. 12, no. 13, pp. 3248–3260, Jul. 2018, doi: 10.1049/iet-gtd.2017.1087.

[19] D. Izci, "A novel improved atom search optimization algorithm for designing power system stabilizer," *Evol. Intell.*, vol. 15, no. 3, pp. 2089–2103, Sep. 2022, doi: 10.1007/s12065-021-00615-9. no. 0123456789, 2021

[20] M. A. El-Dabah, S. Kamel, M. A. Y. Abido, and B. Khan, "Optimal tuning of fractional-order proportional, integral, derivative and tilt-integral-derivative based power system stabilizers using Runge Kutta optimizer," *Eng. Rep.*, vol. 4, no. 6, Jun. 2021, Art. no. e12492, doi: 10.1002/eng2.12492.

[21] Y. L. Abdel-Magid and M. A. Abido, "Optimal multiobjective design of robust power system stabilizers using genetic algorithms," *IEEE Trans. Power Syst.*, vol. 18, no. 3, pp. 1125–1132, Aug. 2003, doi: 10.1109/TPWRS.2003.814848.

[22] S. Ekinci, A. Demiroren, and B. Hekimoglu, "Parameter optimization of power system stabilizers via kidney-inspired algorithm," *Trans. Inst. Meas. Control*, vol. 41, no. 5, pp. 1405–1417, 2019, doi: 10.1177/0142331218780947.

[23] H. Z. A. Kareem, H. H. Mohammed, and A. A. Mohammed, "Robust tuning of power system stabilizer parameters using the modified harmonic search algorithm," *IIUM Eng. J.*, vol. 22, no. 1, pp. 47–57, Jan. 2021, doi: 10.31436/IIUMEJ.V22I1.1276.

[24] A. W. Khawaja, N. A. M. Kamari, and M. A. A. M. Zainuri, "Design of a damping controller using the SCA optimization technique for the improvement of small signal stability of a single machine connected to an infinite bus system," *Energies*, vol. 14, no. 11, p. 2996, May 2021, doi: 10.3390/en14112996.

[25] D. K. Sambariya and R. Prasad, "Design of robust PID power system stabilizer for multimachine power system using HS algorithm," *Amer. J. Elect. Electron. Eng.*, vol. 3, no. 3, pp. 75–82, 2015. [Online]. Available: http://pubs.sciepub.com/ajeee/3/3/3

[26] A. Sabo, N. I. A. Wahab, M. L. Othman, M. Z. A. M. Jaffar, and H. Beiranvand, "Optimal design of power system stabilizer for multimachine power system using farmland fertility algorithm," *Int. Trans. Electr. Energy Syst.*, vol. 30, no. 12, pp. 1–33, Dec. 2020, doi: 10.1002/2050-7038.12657.

[27] A. Sabo, N. I. A. Wahab, M. L. Othman, M. Z. A. M. Jaffar, H. Acikgoz, and H. Beiranvand, "Application of neuro-fuzzy controller to replace SMIB and interconnected multi-machine power system stabilizers," *Sustainability*, vol. 12, no. 22, pp. 1–42, 2020, doi: 10.3390/su12229591.

[28] A. Sabo, N. I. A. Wahab, M. L. Othman, M. Z. A. M. Jaffar, H. Beiranvand, and H. Acikgoz, "Application of a neuro-fuzzy controller for single machine infinite bus power system to damp low-frequency oscillations," *Trans. Inst. Meas. Control*, vol. 43, no. 16, pp. 3633–3646, Dec. 2021, doi: 10.1177/01423312211042781.

[29] A. Sabo, N. I. A. Wahab, M. L. Othman, M. Z. A. B. M. Jaffar, H. Acikgoz, H. Nafisi, and H. Shahinzadeh, "Artificial intelligence-based power system stabilizers for frequency stability enhancement in multi-machine power systems," *IEEE Access*, vol. 9, pp. 166095–166116, 2021, doi: 10.1109/ACCESS.2021.3133285.

[30] D. K. Sambariya and R. Prasad, "Design of optimal proportional integral derivative based power system stabilizer using bat algorithm," *Appl. Comput. Intell. Soft Comput.*, vol. 2016, pp. 1–22, Mar. 2016, doi: 10.1155/2016/8546108.

[31] H. Shayeghi, H. A. Shayanfar, A. Akbarimajd, and A. Ghasemi, "PSS design for a single-machine power system using honey bee mating optimization," in *Proc. Int. Conf. Artif. Intell. (ICAI)*, vol. 1, Jan. 2011, pp. 210–216.

[32] H. Shayeghi, H. A. Shayanfar, S. Asefi, and A. Younesi, "Optimal tuning and comparison of different power system stabilizers using different performance Indices via Jaya algorithm," in *Proc. Int. Conf. Sci. Comput. (CSC)*, vol. 2018, 2016, pp. 34–40.

[33] B. M. Alshammari, A. Farah, K. Alqunun, and T. Guesmi, "Robust design of dual-input power system stabilizer using chaotic Jaya algorithm," *Energies*, vol. 14, no. 17, p. 5294, Aug. 2021, doi: 10.3390/en14175294.

[34] H. Shayeghi, S. Asefi, and A. Younesi, "Tuning and comparing different power system stabilizers using different performance indices applying GWO algorithm," in *Proc. Int. Comprehensive Competition Conf. Eng. Sci.*, vol. 8, 2016, pp. 1–16.

[35] M. Shafiullah, M. J. Rana, L. S. Coelho, and M. A. Abido, "Power system stability enhancement by designing optimal PSS employing backtracking search algorithm," in *Proc. 6th Int. Conf. Clean Electr. Power (ICCEP)*, Jun. 2017, pp. 712–719, doi: 10.1109/ICCEP.2017.8004769.

[36] E. S. Ali and S. M. A. Elazim, "Grasshopper optimization approach for power system stabilizers pattern," *Yanbu J. Eng. Sci.*, vol. 17, no. 1, pp. 1–9, Dec. 2021, doi: 10.53370/001c.23729.

[37] A. T. Moghadam, M. Aghahadi, M. Eslami, S. Rashidi, B. Arandian, and S. Nikolovski, "Adaptive rat swarm optimization for optimum tuning of SVC and PSS in a power system," *Int. Trans. Electr. Energy Syst.*, vol. 2022, pp. 1–13, Jan. 2022, doi: 10.1155/2022/4798029.

[38] L. Chaib, A. Choucha, S. Arif, H. G. Zaini, A. El-Fergany, and S. S. M. Ghoneim, "Robust design of power system stabilizers using improved Harris hawk optimizer for interconnected power system," *Sustainability*, vol. 13, no. 21, p. 11776, Oct. 2021, doi: 10.3390/su132111776.

[39] A. Fathy, D. Yousri, H. Rezk, S. B. Thanikanti, and H. M. Hasanien, "A robust fractional-order PID controller based load frequency control using modified hunger games search optimizer," *Energies*, vol. 15, no. 1, p. 361, 2022, doi: 10.3390/en15010361.

[40] M. Khamies, G. Magdy, A. Selim, and S. Kamel, "An improved Rao algorithm for frequency stability enhancement of nonlinear power system interconnected by AC/DC links with high renewables penetration," *Neural Comput. Appl.*, vol. 34, no. 4, pp. 2883–2911, Feb. 2022, doi: 10.1007/s00521-021-06545-y.

[41] H. M. Hasanien and A. A. El-Fergany, "Salp swarm algorithm-based optimal load frequency control of hybrid renewable power systems with communication delay and excitation cross-coupling effect," *Electr. Power Syst. Res.*, vol. 176, Nov. 2019, Art. no. 105938, doi: 10.1016/j.epsr.2019.105938.

[42] M. Regad, M. Helaimi, R. Taleb, H. A. Gabbar, and A. M. Othman, "Fractional order PID control of hybrid power system with renewable generation using genetic algorithm," in *Proc. IEEE 7th Int. Conf. Smart Energy Grid Eng. (SEGE)*, Aug. 2019, pp. 139–144, doi: 10.1109/SEGE.2019.8859970.

[43] M. Bhuyan, D. C. Das, and A. K. Barik, "Proficient power control strategy for combined solar gas turbine-wind turbine generator-biodiesel generator based two area interconnected microgrid employed with DC link using Harris's hawk optimization optimised tilt-integral-derivative controller," *Int. J. Numer. Model., Electron. Netw., Devices Fields*, vol. 35, no. 4, p. e2991, Jul. 2022, doi: 10.1002/jnm.2991.

[44] N. K. Jena, S. Sahoo, B. K. Sahu, J. Ranjan Nayak, and K. B. Mohanty, "Fuzzy adaptive selfish herd optimization based optimal sliding mode controller for frequency stability enhancement of a microgrid," *Eng. Sci. Technol., Int. J.*, vol. 33, Sep. 2022, Art. no. 101071, doi: 10.1016/j.jestch.2021.10.003.

[45] A. K. Barik, S. Jaiswal, and D. C. Das, "Recent trends and development in hybrid microgrid: A review on energy resource planning and control," *Int. J. Sustain. Energy*, vol. 41, no. 4, pp. 308–322, Apr. 2022, doi: 10.1080/14786451.2021.1910698.

[46] D. H. Wolper and W. G. Macready, "No free lunch theorems for optimization," *IEEE Trans. Evol. Comput.*, vol. 1, no. 1, pp. 67–82, Apr. 1997, doi: 10.1109/4235.585893.

[47] B. Abdollahzadeh, F. S. Gharehchopogh, and S. Mirjalili, "Artificial gorilla troops optimizer: A new nature-inspired metaheuristic algorithm for global optimization problems," *Int. J. Intell. Syst.*, vol. 36, no. 10, pp. 5887–5958, 2021, doi: 10.1002/int.22535.

[48] M. Shafiullah, M. J. Rana, M. S. Alam, and M. A. Abido, "Online tuning of power system stabilizer employing genetic programming for stability enhancement," *J. Electr. Syst. Inf. Technol.*, vol. 5, no. 3, pp. 287–299, Dec. 2018, doi: 10.1016/j.jesit.2018.03.007.

[49] P. Benioff, "The computer as a physical system: A microscopic quantum mechanical Hamiltonian model of computers as represented by Turing machines," *J. Stat. Phys.*, vol. 22, no. 5, pp. 563–591, May 1980, doi: 10.1007/BF01011339.

[50] K.-H. Han and J.-H. Kim, "Quantum-inspired evolutionary algorithm for a class of combinatorial optimization," *IEEE Trans. Evol. Comput.*, vol. 6, no. 6, pp. 580–593, Dec. 2002, doi: 10.1109/TEVC.2002.804320.

[51] J. G. Vlachogiannis and J. Østergaard, "Reactive power and voltage control based on general quantum genetic algorithms," *Expert Syst. Appl.*, vol. 36, no. 3, pp. 6118–6126, Apr. 2009, doi: 10.1016/j.eswa.2008.07.070.

[52] P. Wang, K. Cheng, Y. Huang, B. Li, X. Ye, and X. Chen, "Multi-scale quantum harmonic oscillator algorithm for multimodal optimization," *Comput. Intell. Neurosci.*, vol. 2018, pp. 1–12, May 2018, doi: 10.1155/2018/8430175.

[53] H. A. El-Sattar, S. Kamel, M. H. Hassan, and F. Jurado, "Optimal sizing of an off-grid hybrid photovoltaic/biomass gasifier/battery system using a quantum model of Runge Kutta algorithm," *Energy Convers. Manage.*, vol. 258, Apr. 2022, Art. no. 115539, doi: 10.1016/j.enconman.2022.115539.
[54] G. I. Sayed, G. Khoriba, and M. H. Haggag, "Hybrid quantum salp swarm algorithm for contrast enhancement of natural images," *Int. J. Intell. Eng. Syst.*, vol. 12, no. 6, pp. 225–235, Dec. 2019, doi: 10.22266/IJIES2019.1231.22.
[55] A. H. A. Elkasem, M. Khamies, M. H. Hassan, A. M. Agwa, and S. Kamel, "Optimal design of TD-TI controller for LFC considering renewables penetration by an improved chaos game optimizer," *Fractal Fractional*, vol. 6, no. 4, p. 220, Apr. 2022, doi: 10.3390/fractalfract6040220.
[56] D. Mohammadi, M. A. Elaziz, R. Moghdani, E. Demir, and S. Mirjalili, "Quantum Henry gas solubility optimization algorithm for global optimization," *Eng. Comput.*, pp. 1–20, Mar. 2021, doi: 10.1007/s00366-021-01347-1.
[57] L. S. D. Coelho, "A quantum particle swarm optimizer with chaotic mutation operator," *Chaos, Solitons Fractals*, vol. 37, no. 5, pp. 1409–1418, Sep. 2008, doi: 10.1016/j.chaos.2006.10.028.
[58] W. Zhao, L. Wang, and S. Mirjalili, "Artificial hummingbird algorithm: A new bio-inspired optimizer with its engineering applications," *Comput. Methods Appl. Mech. Eng.*, vol. 388, Jan. 2022, Art. no. 114194, doi: 10.1016/j.cma.2021.114194.
[59] W. Zhao, L. Wang, and Z. Zhang, "Supply-demand-based optimization: A novel economics-inspired algorithm for global optimization," *IEEE Access*, vol. 7, pp. 73182–73206, 2019, doi: 10.1109/ACCESS.2019.2918753.
[60] S. Mirjalili, S. M. Mirjalili, and A. Lewis, "Grey wolf optimizer," *Adv. Eng. Softw.*, vol. 69, pp. 46–61, Mar. 2014, doi: 10.1016/j.advengsoft.2013.12.007.

MAHMOUD A. EL-DABAH was born at Kafr El-Shaikh, in 1985. He received the B.Sc., M.Sc., and Ph.D. degrees from the Faculty of Engineering, Al-Azhar University, Cairo, Egypt, in 2007, 2012, and 2016, respectively. He is an Associate Professor with the Electrical Engineering Department, Faculty of Engineering, Al-Azhar University. His research interests include power systems operation, control, planning, optimization, and renewable energy resources integration in electrical power systems. He is a Reviewer for several journals such as IEEE Access, *Energies*, and IET and different springer nature journals.

MOHAMED H. HASSAN received the M.Sc. degree in electrical engineering from Cairo University, Egypt, in 2018. He is currently pursuing the Ph.D. degree in electrical engineering with Aswan University, Egypt. His research interests include optimization techniques, renewable energy, and smart grids.

SALAH KAMEL received the joint Ph.D. degree from the University of Jaén, Spain, and Aalborg University, Denmark, in January 2014. He is an Associate Professor with the Electrical Engineering Department, Aswan University. He is a Leader of the Power Systems Research Group at the Advanced Power Systems Research Laboratory (APSR Lab), Aswan, Egypt. His research interests include power systems analysis and optimization, smart grid, and renewable energy systems.

HOSSAM M. ZAWBAA received the B.Sc. and M.Sc. degrees from the Faculty of Computers and Information, Cairo University, Giza, Egypt, in 2008 and 2012, respectively, and the Ph.D. degree from Babeş-Bolyai University, Cluj-Napoca, Romania, in 2018. He is currently an Assistant Professor with the Faculty of Computers and Artificial Intelligence, Beni-Suef University, Beni Suef, Egypt. He has over 85 research publications in peer-reviewed reputed journals and international conference proceedings. His research interests include computational intelligence, machine learning, computer vision, and natural language understanding. He was rated as one of the top 2% scientists worldwide by Stanford in the field of AI, in 2020 and 2021. He has been awarded the State Encouragement Award for the year 2020 in the field of Engineering Sciences from the Academy of Scientific Research and Technology, Egypt.